ЗАПОВІДНА СПРАВА

https://doi.org/10.26565/1992-4224-2026-45-13
UDC: 338.49: 656.2: 504.5

L. A. HOROSHKOVA, DSc (Economy), Prof.,
Professor of the Department of Ecology
e-mail: goroshkova69@gmail.com ORCID ID: https://orcid.org/0000-0002-7142-4308
National university of "Kyiv-Mohyla academy"
2, Skovorody, Str., Kyiv, 04070, Ukraine

O. I. MENSHOV, DSc (Geology),
Senior Researcher of the Department of Geoinformatics
e-mail: menshov@knu.ua ORCID ID: https://orcid.org/0000-0001-7280-8453
Taras Shevchenko National University of Kyiv
60, Volodymyrska Str., Kyiv, 01033, Ukraine

D. V. MASLOV,
PhD Student of the Department of Ecology
e-mail: 20denismaslov@gmail.com ORCID ID: https://orcid.org/0009-0009-7397-8329
National university of "Kyiv-Mohyla academy"
2, Skovorody, Str., Kyiv 04070, Ukraine

ASSESSMENT OF MILITARY IMPACTS ON PROTECTED AREAS OF UKRAINE USING SENTINEL-1 AND MACHINE LEARNING

Purpose. To assess military impacts on protected areas of Ukraine using Sentinel-1 Radar Vegetation Index (RVI) data and machine learning methods in order to identify spatial and temporal patterns of vegetation disturbance and ecosystem transformation under wartime conditions

Methods. Spatial and temporal changes are analyzed using remote sensing techniques combined with machine learning methods, including unsupervised classification algorithms to detect patterns of vegetation disturbance and ecosystem transformation. Additionally, comparative analysis and time-series analysis are applied to assess the impact of military activities on forest ecosystems under wartime conditions.

Results. This study assesses the impact of military activity on forest ecosystems in eastern Ukraine using Sentinel-1 SAR data, the Radar Vegetation Index (RVI), baseline-relative change analysis, and unsupervised machine learning. The primary objective was to detect, quantify, and characterize war-related forest disturbance in the Serebrianskyi Botanical Reserve which is directly exposed to active military operations and to understand the extent, severity, and temporal dynamics of that damage relative to a pre-conflict baseline. A conflict-free control site, Homilsha Forests National Nature Park, was used to distinguish military-driven change from background ecological variability. The study addresses whether Sentinel-1 RVI, VV, and VH backscatter can capture the spatial patterns and progressive development of military-induced forest disturbance over the period 2020–2025. Sentinel-1 data were processed in Google Earth Engine and restricted to forest pixels using a land-cover mask. Annual summer composites were generated for each year, and a pre-conflict baseline (2020–2021) was used to quantify post-disturbance change. The analysis encompassed annual RVI trend assessment, rule-based damage classification, K-means clustering, and detection of isolated forest anomalies. After 2022, Serebrianskyi ROI showed a marked RVI decline from stable values in 2020–2022, with changed forest pixels in 2025, including severely disturbed pixels increasing. Homilsha ROI remained stable, and no deterioration trend. Machine-learning results were consistent.

Conclusions. SAR methods have proven to be effective for remote monitoring with limited field access, although derived categories of damage should be interpreted as remote sensing indicators and not as field validated categories of damage.

KEYWORDS: *Sentinel-1, SAR, Radar Vegetation Index, Forest disturbance, affected forests, Remote sensing, Machine learning*

Як цитувати: Horoshkova L.A., Menshov O. I., Maslov D. V. Assessment of military impacts on protected areas of Ukraine using Sentinel-1 and machine learning. *Людина та довкілля. Проблеми неоекології.* 2026. Вип. 45. С. 163-187. https://doi.org/10.26565/1992-4224-2026-45-13

In cites: Horoshkova, L.A., Menshov, O. I., & Maslov D. V. (2026). Assessment of military impacts on protected areas of Ukraine using Sentinel-1 and machine learning. *Man and Environment. Issues of Neoecology,* (43), 163-187. https://doi.org/10.26565/1992-4224-2026-45-13

Introduction

The full-scale military aggression against Ukraine has caused unprecedented environmental damage, particularly within protected natural areas that play a crucial role in preserving biodiversity, maintaining ecosystem stability, and supporting ecological secu-rity. Military operations, including shelling, explosions, fires, fortification construction, and the movement of heavy military equipment, have significantly transformed natural landscapes and accelerated ecosystem degradation. Forest ecosystems located within protected areas are especially vulnerable to such disturbances due to their sensitivity to physical destruction, pyrogenic impacts, and long-term changes in vegetation structure [1, 2].

Armed conflict is increasingly recognized as a major cause of environmental degradation, forest degradation, biodiversity loss and land cover change. The environmental impacts of war are both direct and indirect. Direct impacts include shelling, explosions, fire, bombing, movement of military vehicles, trench construction, fortification construction and deliberate destruction of vegetation. Indirect impacts include illegal logging, resource extraction driven by displacement, reduced forest management, weakened conservation enforcement, limited access to monitoring and loss of forest management capacity [3-5] defines the field as the ecology of war, and stresses that war should be understood not only as a political or humanitarian crisis, but also as a process of environmental degradation. This aspect is particularly important in forested conflict zones where repeated disturbance can change the structure of vegetation, soil characteristics, etc.

Military activity may affect forest ecosystems through a number of interacting pathways. Explosions and artillery fire can break the stems, damage the crowns, create craters, ignite the fires, and expose the bare ground. Heavy military vehicles can compact the soil, disturb the roots, damage the undergrowth and create trails that fragment the forest habitat. Trenching, building of roads and fortification may further alter the microtopography, drainage and continuity of forests. In addition, limited access during conflict can hinder firefighting, pest control, sanitary logging, biodiversity monitoring and restoration activities [4, 6]. These processes can result in canopy degradation, biomass loss, fire scars, soil disturbance, fragmentation, pollution and long-term loss of environmental resilience.

The link between armed conflict and forests is complex, as war can have a wide range of environmental impacts depending on the intensity of the conflict, governance conditions, displacement of populations and the demand for resources. McNeely (2003) describes how forest biodiversity is directly affected by the destruction of habitats and indirectly by institutional collapse or increased exploitation. Gaynor, et al. [7] goes on to explain that armed conflict can have multiple impacts on conservation, such as mortality of wildlife, loss of habitats, displacement and changes in human pressure. Armed conflicts may lead to rapid forest loss through logging, mining, fires and military damage, or they may restrict certain uses by trade or access restrictions [8]. Conflict-related changes in forests should therefore be assessed with regard to local ecological conditions, the basic vegetation structure, the exposure to conflict and the comparison areas.

Comparative evidence from other conflicts shows different environmental damage caused by war. During the Vietnam War, forests were severely damaged by chemical pollution, bombing, fire, and long-term contamination, making Vietnam one of the most notorious examples of environmental degradation caused by military action [3, 6]. In Syria, war-related deforestation is associated with fuel wood extraction, displacement, administrative collapse and displacement through direct famines, Daiyoub et al. [9] using remote sensing and machine learning to detect conflict forest extinctions from 2010 to 2019. n the Democratic Republic of Congo, Butsic et al. [10] found that warfare, mining, and protected areas interacted to shape deforestation patterns. In Rwanda, Ordway [8] has shown that

post-conflict forest outcomes can be politically and institutionally complex, with changes in forests shaped by both conflict-induced destruction and post-conflict conservation policies. These examples show that the environmental damage caused by conflict may include canopy loss, deforestation, loss of biodiversity, soil degradation, pollution, altered fire regimes, fragmentation of habitats and weakened environmental governance. Remote sensing has become a central tool for assessing environmental damage in war-affected regions because field surveys are often unsafe, delayed, or impossible. Kaplan et al. [11] reviewed the usage of remote sensing for environmental protection in war situations and demonstrated that satellite data can be used to support the assessment of forest loss, fire, soil degradation, oil pollution, damage to infrastructure and damage to agriculture. Shevchuk et al. [12] used remote sensing data to investigate environmental consequences of the Russia–Ukraine war and emphasized the importance of satellite monitoring where field access is limited. More generally, remote conflict monitoring is becoming more widespread as high-resolution satellite imagery, dense time series data and machine learning technologies become more available [13]. Remote sensing is therefore valuable not only for detecting physical damage, but also for producing replicable evidence that can be compared with comparable evidence from other times and other places.

Optical sensors such as Landsat and Sentinel-2 are widely used to monitor vegetation loss, burn scars, changes in soil cover and the decline of forests. However, optical images are limited by cloud cover, smoke, seasonal lighting and atmospheric conditions. Synthetic aperture radar (SAR), in particular Sentinel-1, is an important addition as it can receive data without interference from daylight and is less affected by cloud cover. The SAR backscatter is sensitive to the structure of vegetation, humidity, surface roughness and geometry of the canopy, which makes it suitable for monitoring forests under challenging observation conditions [14-17]. This makes Sentinel-1 particularly useful in conflict-affected areas where it is necessary to monitor continuously and where optical images may be incomplete.

The vegetation index of the radar scan is commonly used to summarize the vegetation scatter. In the Sentinel-1 dual-polarization data, VH backscattering is generally related to volume scattering from vegetation canopy, whereas VV backscattering is more affected by surface scattering and double-spreading effects. The RVI combines these signals to represent the density of vegetation, the structure of the canopy and the characteristics related to biomass. Mandal et al. [14] demonstrated the value of the dual polarimetric RVI for vegetation monitoring by using Sentinel-1 SAR data. Vreugdenhil et al. [16] explored the relationship between the Sentinel-1 ratio metrics and optical depth of vegetation in Europe. These studies support the use of vegetation indices derived from the SAR for the detection of changes in vegetation structure where optical data alone may not be sufficient.

In forest ecosystems, SAR-based monitoring is particularly useful because structural disturbance may occur before complete land-cover conversion. Forest degradation may involve partial canopy loss, branch breakage, reduced understory complexity, soil exposure, or burn effects without immediate conversion to non-forest land cover. Optical vegetation indices can detect greenness and photosynthetic activity, but SAR can add information on canopy structure, moisture, and surface conditions. Studies combining SAR and optical time series have shown that multi-source approaches improve disturbance mapping and forest monitoring, particularly in heterogeneous landscapes [18-20]. For conflict-affected forests, this is important because war-related disturbance may be spatially irregular, temporally abrupt, and structurally complex.

Machine learning has also become increasingly important in forest monitoring and conflict-related environmental assessment. In many conflict zones, field reference data are limited or unavailable, making unsupervised, weakly supervised, or semi-supervised approaches useful. Clustering methods can identify groups of pixels with similar temporal or structural characteristics, while anomaly detection can highlight observations that depart from expected behavior. Daiyoub et al. [9] used remote sensing and machine learning to assess war-induced deforestation in Syria, and Gatti et al. [21] applied machine learning to detect forest loss in Ukraine during the war. More generally, machine-learning approaches have been widely used with Sentinel-1 and Sentinel-2 data for land-cover mapping, biomass estimation, disturbance detection, and forest monitoring [18, 22, 23].

For conflict-affected forests, an integrated approach combining SAR indices, temporal baselines, control areas, and machine-learning classification is methodologically valuable. Baseline comparison helps distinguish disturbance from normal seasonal variability, while control areas provide a reference for regional environmental variation. Machine learning can support classification of forest condition where field labels are limited. However, remote-sensing-derived damage classes should be interpreted as indicators of structural disturbance rather than direct field-confirmed damage categories. SAR signals can be influenced by canopy structure, moisture, surface roughness, burn effects, and acquisition geometry. Therefore, the strongest interpretation comes from convergence among multiple indicators, such as temporal change, spatial pattern, SAR backscatter, vegetation indices, and contextual evidence of conflict exposure.

In the context of conflict-related ecological assessment, the major expected damage types from military activity include canopy degradation, tree mortality, burned vegetation, fragmentation, soil compaction, crater formation, trench disturbance, altered hydrology, contamination, and restricted forest recovery.

Compared with cases such as Vietnam, Syria, the Democratic Republic of Congo, and Rwanda, forest disturbance in Ukraine should be understood within a combined framework of direct military pressure, protected-area vulnerability, remote-sensing detectability, and limited field access.

The use of Sentinel-1 RVI and machine-learning methods therefore contributes to a growing body of research that uses Earth observation to assess ecological damage in conflict-affected regions. In relation to the present article, this literature supports the methodological use of Sentinel-1 SAR, RVI, baseline-relative change analysis, and unsupervised machine learning for forest disturbance assessment in areas where military activity limits direct ecological fieldwork.

Objects and Research Methods

Study Area. This study focuses on two forest regions defined as areas of interest (AOIs) in eastern Ukraine (fig. 1) representing different levels of exposure to disturbance associated with military activity. The first AOI corresponds to the Serebrianskyi Botanical Reserve, located within the Kreminna forest massif in Luhansk region. The reserve is situated approximately 8 km southwest of the city of Kreminna, within the Kreminna district, and encompasses forest compartments 110–113 and 131 of the Serebrianka forestry of the State Enterprise "Kreminna Forestry and Hunting Range". This AOI is located in close proximity to the active frontline and has been directly affected by warfare, military operations, and associated disturbances since 2022. The second AOI is located within Homilsha Forests National Nature Park in Kharkiv region and lies at a greater distance from the frontline, with comparatively lower exposure to direct military activity during the same period. The spatial configuration of both AOIs and their relative position with respect to the frontline are illustrated in Figure 1, where the Serebrianskyi AOI (Serebrianka forest area) is highlighted in red and the Homilsha AOI is shown in blue.

The Serebrianskyi AOI was defined as a rectangular polygon (38.1125–38.2375°E, 48.96–49.02°N), representing a forested area adjacent to zones of active hostilities. The Homilsha AOI was delineated as a polygon derived from a 2.5 km buffer around a central coordinate (36.2796°E, 49.5939°N), capturing a forest area spatially separated from the main conflict zone. To ensure consistency in land cover conditions for remote sensing analysis, both AOIs were restricted to forested pixels using the ESA WorldCover 2020 dataset (forest class = 10). A spatial connectivity filter (minimum of 8 connected pixels) was further applied to exclude isolated or potentially misclassified pixels, thereby retaining only contiguous forest patches suitable for analysis. These preprocessing steps ensure that subsequent analysis is limited to structurally consistent forest areas.

Syntaxonomic Composition and Structural Characteristics of Forest Vegetation in the Study Areas. The Serebrianskyi Botanical Reserve (Kreminna forest massif) is characterized by forest vegetation belonging mainly to the classes Vaccinio-Piceetea (pine forests on sandy substrates) and Quercetea robori-petraeae (oak-dominated forests), including alliances such as Dicrano-Pinion sylvestris and Querco roboris-Pinion sylvestris. The vegetation is dominated by Pinus sylvestris and Quercus robur, with admixture of Betula pendula, Populus

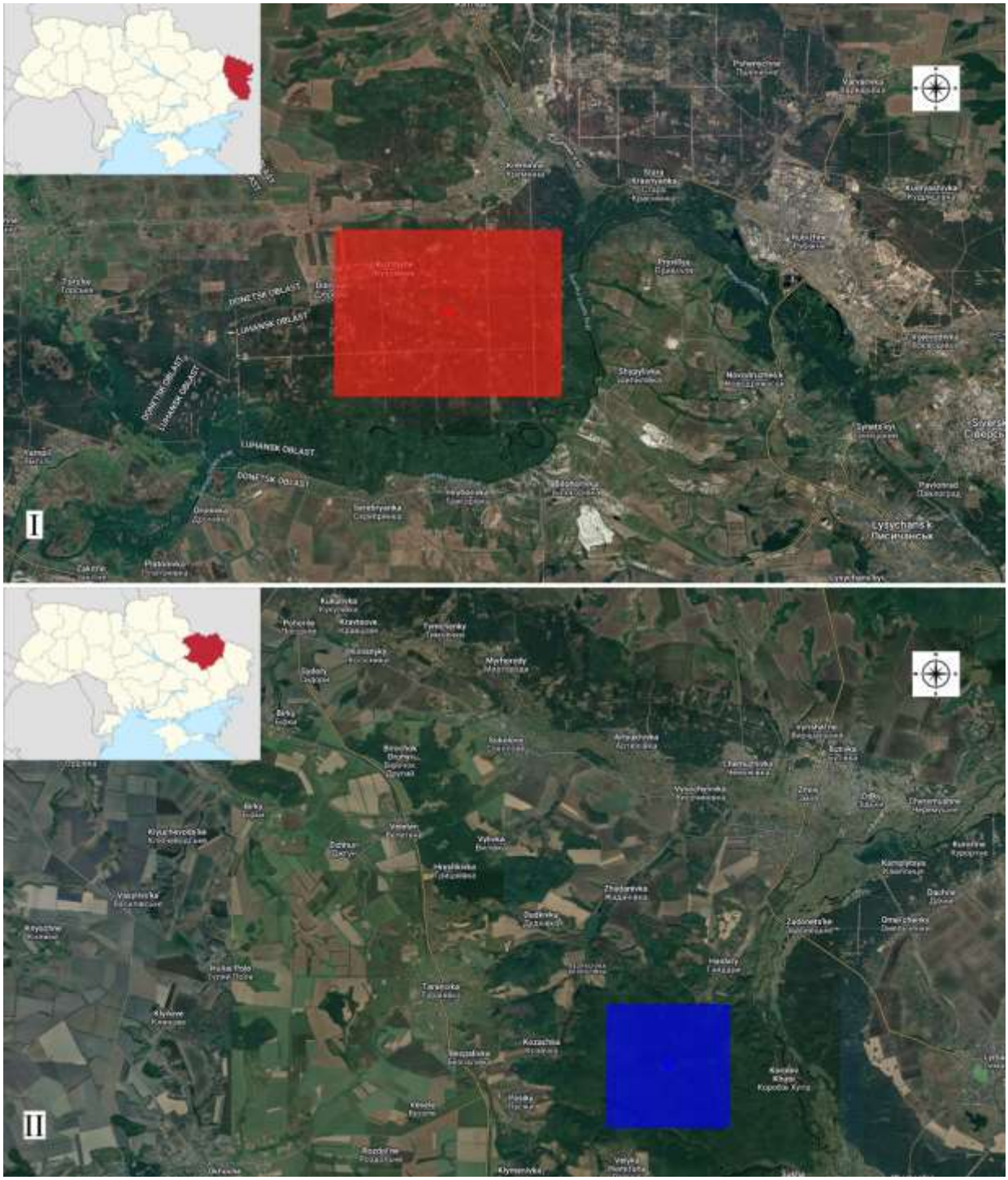

Fig. 1 – Study areas used in the analysis: (top) *Serebrianskyi Botanical Reserve AOI* (Serebrianka forest area, Luhansk region) shown as a red polygon located near the frontline and exposed to active military operations; (bottom) *Homilsha Forests AOI* (Kharkiv region) shown as a blue polygon, located farther from the frontline with lower exposure to direct military activity

tremula, and occasionally Acer platanoides. The ground layer typically includes Calamagrostis epigejos, Festuca ovina, Carex ericetorum, Convallaria majalis, and Polygonatum odoratum, along with lichens of the genus Cladonia and mosses such as Pleurozium schreberi and Dicranum. Structurally, these forests are usually two-layered, with a pine-dominated canopy on nutrient-poor sandy soils and a relatively sparse herbaceous layer composed of xerophilous and

forest-steppe species. Lichen and moss cover can be well developed in more open stands, reflecting dry edaphic conditions typical of river terrace ecosystems in the Siverskyi Donets basin.

The Homilsha Forests National Nature Park (Kharkiv region) represents mesophytic broadleaved and mixed forests of the forest-steppe zone, primarily associated with the class Quercetea robori-petraeae and, locally, Vaccinio-Piceetea in pine-dominated areas. The dominant tree species are Quercus robur and Pinus sylvestris, accompanied by Acer platanoides, Tilia cordata, Fraxinus excelsior, and Betula pendula. The herbaceous layer is comparatively species-rich, including Aegopodium podagraria, Stellaria holostea, Carex pilosa, Asarum europaeum, and Convallaria majalis, while the moss layer is less pronounced and composed mainly of mesophytic forest species such as Brachythecium. These forests exhibit a well-developed multi-layered structure with a dense canopy, distinct shrub layer, and diverse understory, reflecting more favorable moisture conditions and higher ecological stability compared to the Serebrianskyi AOI.

Satellite Data, Preprocessing, and Radar Vegetation Index. Vegetation monitoring is commonly performed using optical remote sensing data; however, optical observations are limited by cloud cover and illumination conditions. These limitations reduce data availability, especially in regions affected by warfare and military activity, where continuous monitoring is required. To address this, this study uses Synthetic Aperture Radar (SAR) data from the Copernicus Sentinel-1 mission, which provides observations independent of atmospheric conditions and solar illumination.

Sentinel-1 Ground Range Detected (GRD) products were processed in Google Earth Engine (GEE). Data selection was limited to the Interferometric Wide (IW) acquisition mode with dual polarization (VV and VH), covering the period from January 2020 to December 2025. Both ascending and descending orbit passes were included to increase temporal coverage and reduce acquisition bias.

The two polarizations provide different information about surface and vegetation structure. VV polarization is mainly sensitive to surface scattering and double-bounce effects, while VH polarization is more sensitive to volume scattering within vegetation canopies.

Preprocessing was applied to ensure consistency of the SAR data. Standard Sentinel-1 processing includes orbit file application, thermal noise removal, radiometric calibration, and terrain correction (fig. 2).

After preprocessing, the data were prepared for analysis. The processed images were spatially subset to the defined AOIs. The VV and VH polarization bands were then separated and transformed between linear and decibel representations as required for further processing (fig. 3).

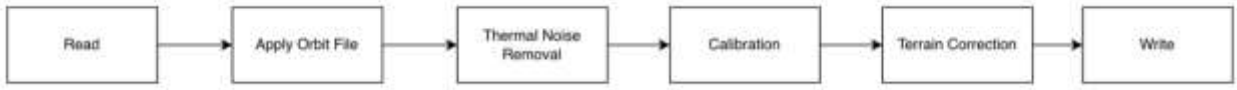

Fig. 2 – Sentinel-1 preprocessing workflow including orbit file application, thermal noise removal, radiometric calibration, and terrain correction

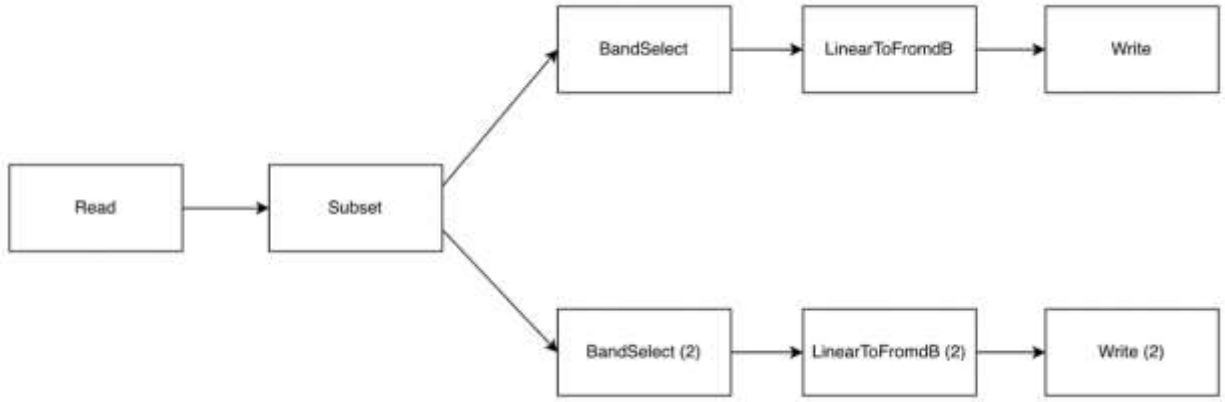

Fig. 3 – Post-processing workflow including spatial subsetting to AOIs, separation of VV and VH bands, and conversion between linear and decibel backscatter values

Vegetation dynamics were quantified using the **Radar Vegetation Index (RVI)**. The RVI was calculated for each Sentinel-1 acquisition as:

$$RVI = \frac{4 \cdot \sigma^0_{VH}}{\sigma^0_{VV} + \sigma^0_{VH}}$$

where σ^0VV and σ^0VH represent the backscatter coefficients in the co-polarized (vertical transmit–vertical receive) and cross-polarized (vertical transmit–horizontal receive) channels, respectively. The RVI exploits the sensitivity of cross-polarized backscatter (VH) to volume scattering within vegetation canopies, while the co-polarized component (VV) is more influenced by surface and double-bounce scattering.

As a result, higher RVI values generally indicate increased vegetation density, structural complexity, and biomass, whereas lower values correspond to sparse vegetation or non-vegetated surfaces. The normalization by the sum of VV and VH reduces the influence of absolute backscatter intensity and improves comparability across different acquisition conditions.

Time-Series Data Processing. To reduce speckle noise and short-term variability inherent in SAR data, seasonal composites were generated using median aggregation for the peak vegetation period (June–August), with additional emphasis on July–August to enhance interannual contrast. For each year, median composites of VV, VH, the Radar Vegetation Index (RVI), and the VH/VV ratio were produced after applying a forest mask to ensure consistency in land cover. A pre-disturbance baseline was subsequently defined as the mean of the 2020–2021 seasonal composites, providing a stable reference against which anomalies and potential disturbance signals could be evaluated.

A multi-temporal feature stack was constructed at the pixel level to capture both structural properties and temporal dynamics of vegetation. This included baseline features (VV, VH, RVI, and VH/VV ratio), post-disturbance metrics for 2024–2025 (mean values and differences relative to baseline such as ΔRVI, ΔVV, and ΔVH), and temporal statistics for 2022–2025 (mean, minimum, maximum, standard deviation, range, and linear trend of RVI). In addition, annual RVI values from 2020 to 2025 were retained as a time series, alongside a contextual binary indicator distinguishing conflict-affected and control regions, enabling differentiation between disturbance-driven and natural variability.

To ensure computational efficiency while maintaining statistical robustness, a stratified random sampling approach was applied, selecting 12,000 pixels per region at a spatial resolution of 20 m. Sampling was conducted directly on the feature stack while preserving spatial geometry, resulting in a combined dataset of approximately 24,000 forest pixels. Monthly time series of RVI, VV, VH, and the VH/VV ratio were then computed for each region and aggregated over the June–August period to assess seasonal behavior and long-term trends. Annual summary statistics, including mean, median, and upper percentiles (75th and 90th), were also derived, with the optimal reducer selected based on its ability to maximize contrast between disturbed and control areas while minimizing noise.

Integrated Remote Sensing and Machine Learning Pipeline for Forest Disturbance Detection. A structured methodological framework was implemented to detect and classify forest disturbances using SAR-derived indicators. The workflow operates at the pixel level and is based on large-scale sampling of Sentinel-1 data within predefined AOIs. For each region, approximately 12,000 pixels were sampled at 20 m spatial resolution, and a multi-temporal feature dataset was constructed for the period 2020–2025. The analysis focuses on summer months (June–August) to ensure consistency of vegetation conditions and reduce seasonal variability. A baseline period (2020–2021) was defined to represent pre-disturbance conditions, against which subsequent changes were quantified. The workflow integrates SAR preprocessing, feature extraction, temporal analysis, and unsupervised machine learning to derive spatially explicit indicators of forest condition and disturbance.

The analytical workflow presented in Figure 4 follows a structured multi-step pipeline for detecting and classifying forest disturbances using SAR-derived indicators. The process begins with study area definition, where Areas of Interest (AOIs) are delineated and constrained to forest cover. This is followed by data acquisition, where Sentinel-1 SAR imagery (VV and VH polarization) is collected for the period 2020–2025. In the preprocessing stage, the dataset is filtered according to acquisition parameters (date, orbit, polarization), and radiometric and geometric corrections are applied.

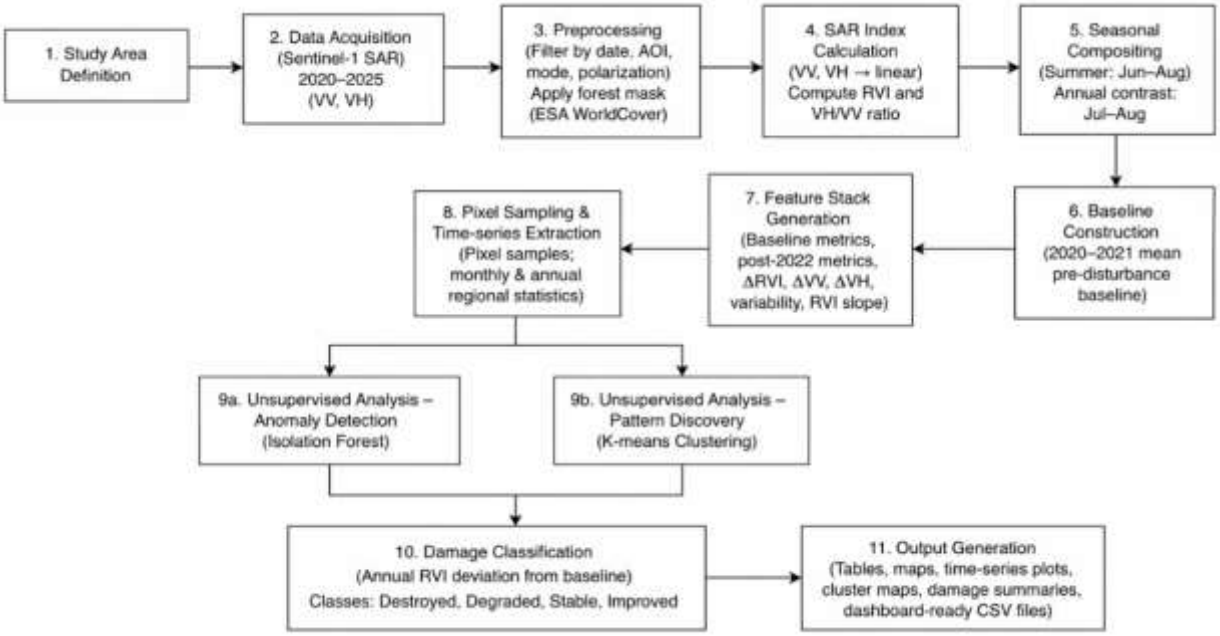

Fig. 4 – SAR-based workflow for forest disturbance detection, including preprocessing, index calculation (RVI, VH/VV), feature generation, unsupervised analysis (K-Means, Isolation Forest), and rule-based classification

After preprocessing, SAR-based indices are computed, including the Radar Vegetation Index (RVI) and the VH/VV ratio, which capture vegetation structure and scattering behavior. These indices form the basis for subsequent temporal analysis. Seasonal compositing is performed to reduce short-term variability and noise. Summer composites (June–August) are used to represent peak vegetation conditions, while inter-annual comparisons focus on consistent seasonal windows. A baseline is then constructed using pre-disturbance observations (2020–2021), providing a reference for detecting deviations in subsequent years. Following baseline definition, a feature stack is generated by combining multiple indicators, including baseline statistics, post-2022 deviations (ΔRVI, ΔVV, ΔVH), temporal trends (e.g., RVI slope), and variability metrics. These features are used as input for pixel-level sampling and time-series extraction, enabling both spatial and temporal analysis. The pipeline then branches into two complementary unsupervised approaches. First, clustering is applied using the K-Means algorithm (clustering module, Scikit-learn) to group pixels into four categories representing different forest condition states. Second, anomaly detection is performed using the Isolation Forest algorithm (ensemble module, Scikit-learn), which identifies pixels exhibiting unusual temporal behavior relative to the overall dataset. The outputs of these analyses are integrated into a damage classification stage, where a rule-based system assigns each pixel to one of four classes (destroyed, degraded, stable, improved) based on deviations from baseline conditions. Finally, the workflow produces spatial and statistical outputs, including disturbance maps, annual summaries, cluster distributions, and time-series visualizations. The entire pipeline was implemented in Python, using the Google Earth Engine API for large-scale data processing, NumPy and Pandas for data handling, Scikit-learn for machine learning (preprocessing, clustering, anomaly detection), and Matplotlib for visualization.

Unsupervised Analysis and Rule-Based Damage Classification. Unsupervised machine learning was selected due to the absence of reliable ground truth data in conflict-affected regions. This approach enables the identification of intrinsic patterns in the data without predefined labels and is therefore suitable for exploratory analysis of disturbance dynamics. Clustering was performed using the K-Means algorithm (clustering module, Scikit-learn), which partitions the feature space into a predefined number of clusters by minimizing within-cluster variance. The number of clusters was set to four, corresponding to an interpretable gradient

of forest condition ranging from intact to severely disturbed. Multiple initializations (n = 20) were used to improve solution stability, and cluster quality was evaluated using the silhouette score. The resulting clusters were interpreted semantically based on their statistical properties, including RVI levels, temporal trends, and variability. Additional interpretation was supported by spatial distribution patterns across AOIs, allowing differentiation between disturbance-related and background variability. In parallel, anomaly detection was conducted using the Isolation Forest algorithm (ensemble module, Scikit-learn). This method identifies observations that are easier to isolate in a random partitioning process, which correspond to rare or unusual patterns in the dataset.

The model was configured with 400 trees and a contamination rate of 12%, producing both anomaly scores and binary labels. This approach is particularly effective for detecting localized or non-systematic disturbances that may not form distinct clusters. To obtain interpretable outputs, a rule-based classification framework was applied to translate continuous change metrics into discrete disturbance classes. The classification is based on deviations of annual RVI values from the baseline, normalized by the standard deviation (σ) of baseline variability. Thresholds were defined using a combination of pixel-level statistics and regional quantile constraints. Specifically, the standard deviation of baseline RVI was used to account for natural variability, while a 90th percentile floor was applied to avoid unrealistically low thresholds in stable areas.

Each pixel-year observation was classified into one of four categories: destroyed ($\Delta RVI < -2\sigma$), degraded ($-2\sigma \leq \Delta RVI < -\sigma$), stable ($|\Delta RVI| \leq \sigma$), and improved ($\Delta RVI > \sigma$). This formulation ensures that classification reflects both the magnitude of change and the inherent variability of the system, improving robustness across heterogeneous conditions.

Results and Discussion

Changes in Sentinel-1 vegetation signal in the conflict-affected and control forests. As shown in Figure 5, the Sentinel-1 results revealed a clear divergence between the conflict-affected Serebrianskyi Botanical Reserve and the control site in Homilsha Forests National Nature Park. During the pre-disturbance period, corresponding to 2020–2022, both regions exhibited relatively stable seasonal behavior, with no pronounced directional change in the mean summer RVI signal. In Serebrianskyi, RVI values remained high and comparatively consistent during this interval, indicating stable canopy-related scattering conditions. In contrast, the Homilsha control site showed only minor interannual variation and no evidence of marked decline.

After 2023, a different pattern became evident. In the Serebrianskyi site, RVI decreased substantially relative to the pre-disturbance baseline, and this decline continued through 2024–2025. The reduction in RVI was accompanied by a concurrent decrease in both VV and VH backscatter, with a more pronounced decline in the cross-polarized VH component. This pattern is consistent with a reduction in volumetric scattering from forest vegetation and suggests a progressive loss of canopy structure. In contrast, the Homilsha site remained comparatively stable over the same period, with only limited fluctuations in backscatter and a slight positive shift in RVI relative to the baseline. The annual values supporting this comparison are summarized in Table 1.

Overall, the contrast between the two AOIs indicates that the observed decline in the conflict-affected forest cannot be explained by regional seasonal variability alone. Because both sites were analyzed using the same seasonal window and processing workflow, the divergence between the two forests provides direct evidence of disturbance-related structural change in the Serebrianskyi forest. These results establish the basis for the subsequent spatial and machine learning analyses.

Annual change in RVI relative to the pre-disturbance baseline. The annualized comparison relative to the 2020–2021 baseline provided a clearer measure of divergence between the two study areas. As shown in Figure 6, both AOIs remained close to baseline conditions during 2020–2022, indicating that no substantial departure from the reference period was evident in the early part of the observation record.

From 2023, the annual pattern differed between the two study areas. In the Serebrianskyi Botanical Reserve, RVI changed from

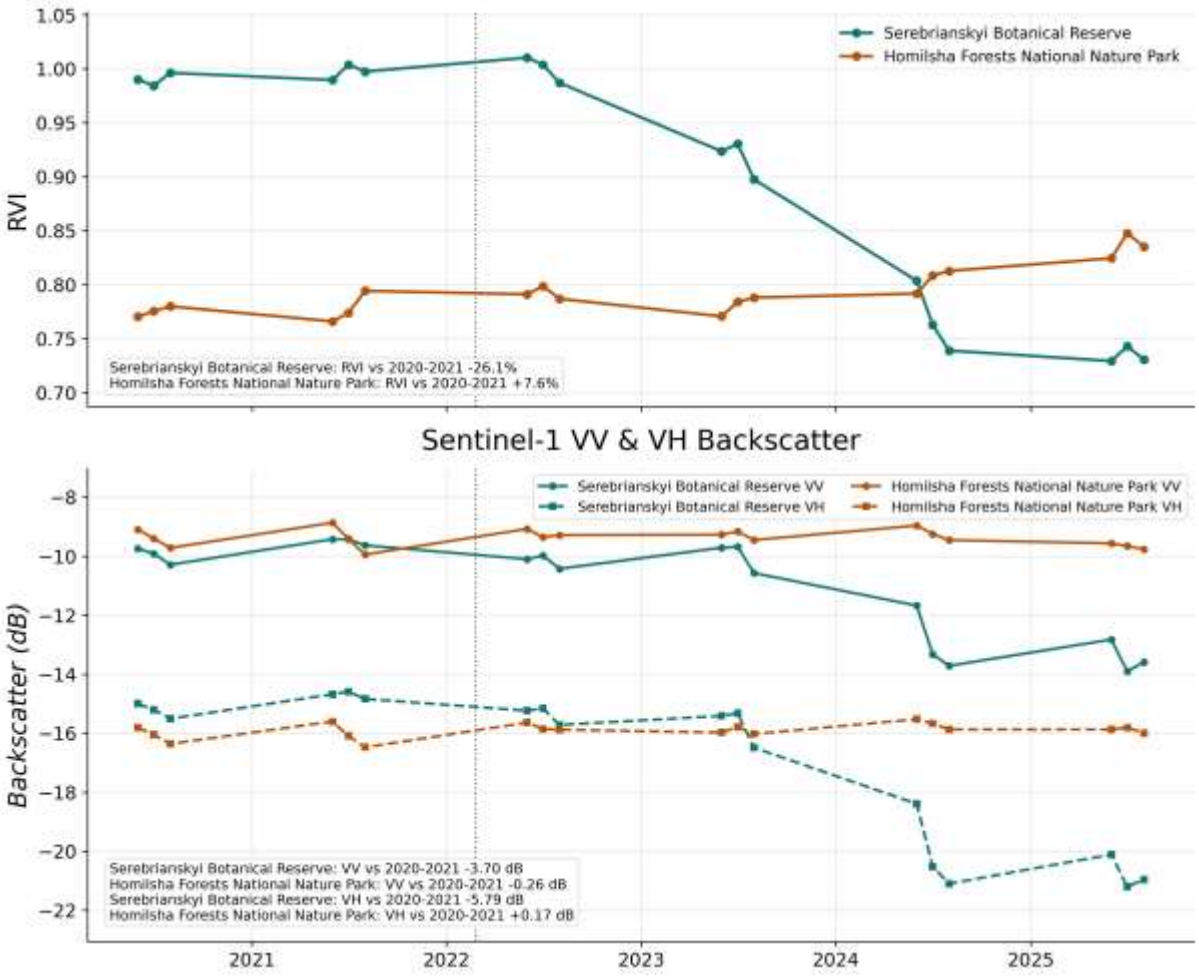

Fig. 5 – Changes in Sentinel-1 Radar Vegetation Index (RVI), VV backscatter, and VH backscatter in the conflict-affected Serebrianskyi Botanical Reserve and the control site in Homilsha Forests National Nature Park during 2020–2025

near-baseline values in 2021–2022 to a negative deviation of about 8.6% in 2023. This decline increased to about 26.6% in 2024 and remained at a similarly low level in 2025, at about 28.7% below the baseline. The largest year-to-year decrease was observed between 2023 and 2024, when the baseline-relative RVI dropped by about 18 percentage points. These results indicate that the main shift in the vegetation signal occurred after 2022 and became substantially stronger in 2024.

In contrast, the Homilsha control site did not show a negative trend. After remaining close to baseline in 2020–2021, it showed a positive deviation of about 2.7% in 2022, a slightly lower but still positive value of about 1.8% in 2023, and further increases to about 5.1% in 2024 and 8.5% in 2025. Thus, while the conflict-affected forest showed a progressive negative shift, the control forest remained stable and showed a small positive change relative to the baseline.

The difference between the two AOIs increased strongly after 2022. In 2023, the separation between the sites was about 10.4 percentage points. This difference increased to about 31.7 percentage points in 2024 and to about 37.2 percentage points in 2025. Therefore, the annual baseline-relative comparison not only confirms the difference observed in the seasonal time series, but also shows that the divergence between the conflict-affected and control forests became larger through time. Overall, the Serebrianskyi site showed a sustained decrease in RVI relative to the pre-disturbance baseline, whereas the Homilsha site remained stable or slightly positive during the same period.

Table 1

Annual Sentinel-1 summer metrics for the conflict-affected and control forest sites during 2020–2025

Region Name	Year	RVI	VV	VH	Ratio
Serebrianskyi Botanical Reserve	2020	0.93	-10.03	-15.23	0.31
	2021	0.94	-9.46	-14.6	0.31
	2022	0.94	-10.07	-15.22	0.31
	2023	0.86	-10.14	-15.85	0.28
	2024	0.69	-13.45	-20.4	0.21
	2025	0.67	-13.83	-20.83	0.2
Homilsha Forests National Nature Park	2020	0.72	-9.5	-16.09	0.22
	2021	0.73	-9.59	-16.15	0.22
	2022	0.74	-9.28	-15.78	0.23
	2023	0.74	-9.24	-15.8	0.23
	2024	0.76	-9.29	-15.67	0.24
	2025	0.78	-9.64	-15.79	0.24

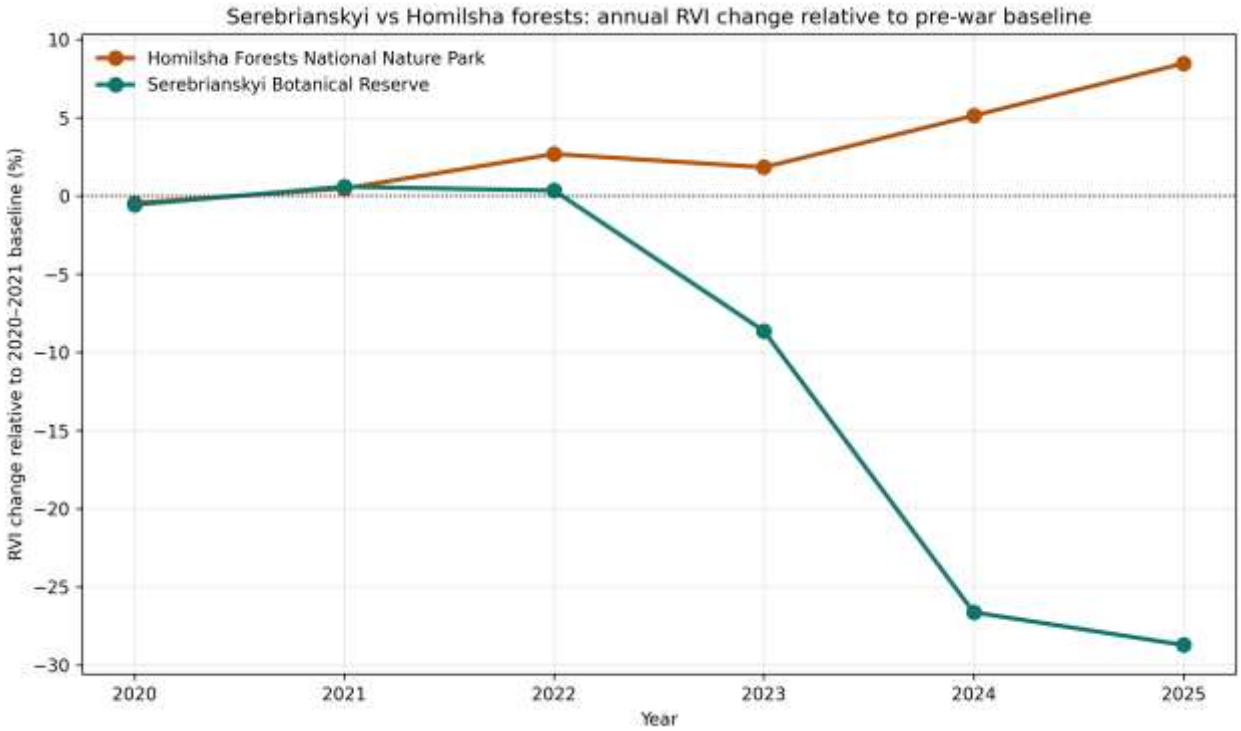

Fig. 6 – Annual change in Radar Vegetation Index (RVI) relative to the 2020–2021 baseline in the conflict-affected Serebrianskyi Botanical Reserve and the control site in Homilsha Forests National Nature Park during 2020–2025

Progressive increase in damaged forest share from 2022 to 2025. The damage classification results showed no measurable damage signal in either study area in 2020–2021. As shown in Figure 7, the share of changed forest pixels, defined as the sum of degraded and destroyed classes, was 0.0% in both regions in both years. In 2022, non-zero values appeared in both sites, with 8.7% changed pixels in the Serebrianskyi Botanical Reserve and 9.4% in the Homilsha control site. However, from 2023 the two study areas showed different patterns.

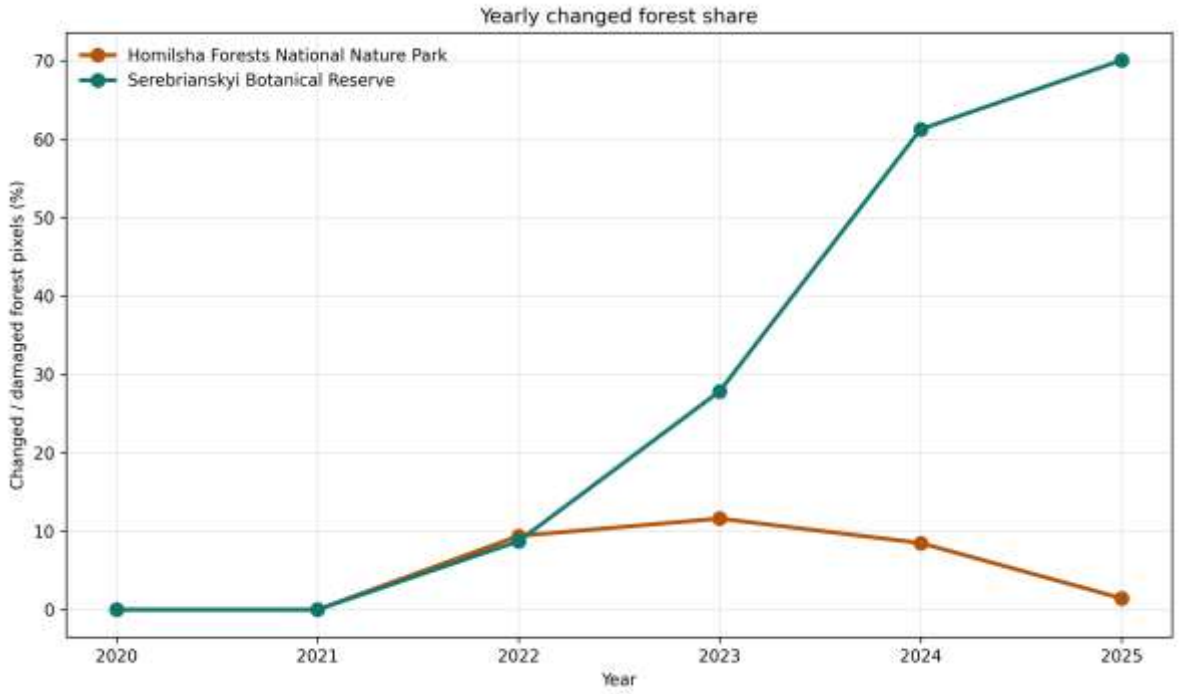

Fig. 7 – Annual share of changed forest pixels (%) in the conflict-affected Serebrianskyi Botanical Reserve and the control site in Homilsha Forests National Nature Park during 2020–2025.

In the Serebrianskyi Botanical Reserve, the share of changed forest increased to 27.9% in 2023, 61.3% in 2024, and 70.1% in 2025. This corresponds to an increase of 19.2 percentage points between 2022 and 2023, followed by a further increase of 33.4 percentage points between 2023 and 2024. The increase from 2024 to 2025 was smaller, at 8.8 percentage points, which indicates persistence of a high damage level after the sharp increase observed in 2024.

A similar pattern was observed for the strongly damaged class. As shown in Figure 8, the share of destroyed forest pixels in the Serebrianskyi Botanical Reserve was 0.0% in 2020–2021, increased to 0.4% in 2022 and 4.9% in 2023, and then rose sharply to 35.7% in 2024 and 42.7% in 2025.

The largest increase occurred between 2023 and 2024, when the destroyed share increased by 30.8 percentage points. This indicates that the rise in total damaged area was associated not only with moderate degradation, but also with a strong increase in the most severe damage class.

The class composition shown in Figure 9 further supports this result. In the Serebrianskyi Botanical Reserve, the stable class decreased from 91.3% in 2022 to 72.2% in 2023, 38.7% in 2024, and 29.9% in 2025. At the same time, the destroyed class increased from 0.4% in 2022 to 4.9% in 2023, 35.7% in 2024, and 42.7% in 2025, while the degraded class increased from 8.3% in 2022 to 23.0% in 2023, 25.6% in 2024, and 27.4% in 2025. These values show a progressive shift from stable forest conditions to damaged classes, with the largest change occurring after 2023.

In contrast, the Homilsha control site did not show the same cumulative increase. The share of changed forest pixels was 9.4% in 2022, 11.6% in 2023, 8.5% in 2024, and 1.4% in 2025. The destroyed class remained low throughout the study period, with values of 0.5%, 0.7%, 0.6%, and 0.0% in 2022–2025, respectively. In the same period, stable and improved classes remained dominant in the control site. Overall, these results show that the decline in the radar vegetation signal in the conflict-affected forest corresponded to a strong increase in damaged forest area, whereas the control site showed only low-level variation without progressive accumulation of damage.

Spatial progression of disturbance across years. The spatial maps showed that the disturbance pattern in the conflict-affected forest was organized in space and changed over time. In 2021, both study areas were assigned almost entirely to the stable/improved class. No degraded or destroyed zones were identified in either AOI, and the spatial pattern was uniform in both forests. This pre-disturbance condition is shown in Figure 10.

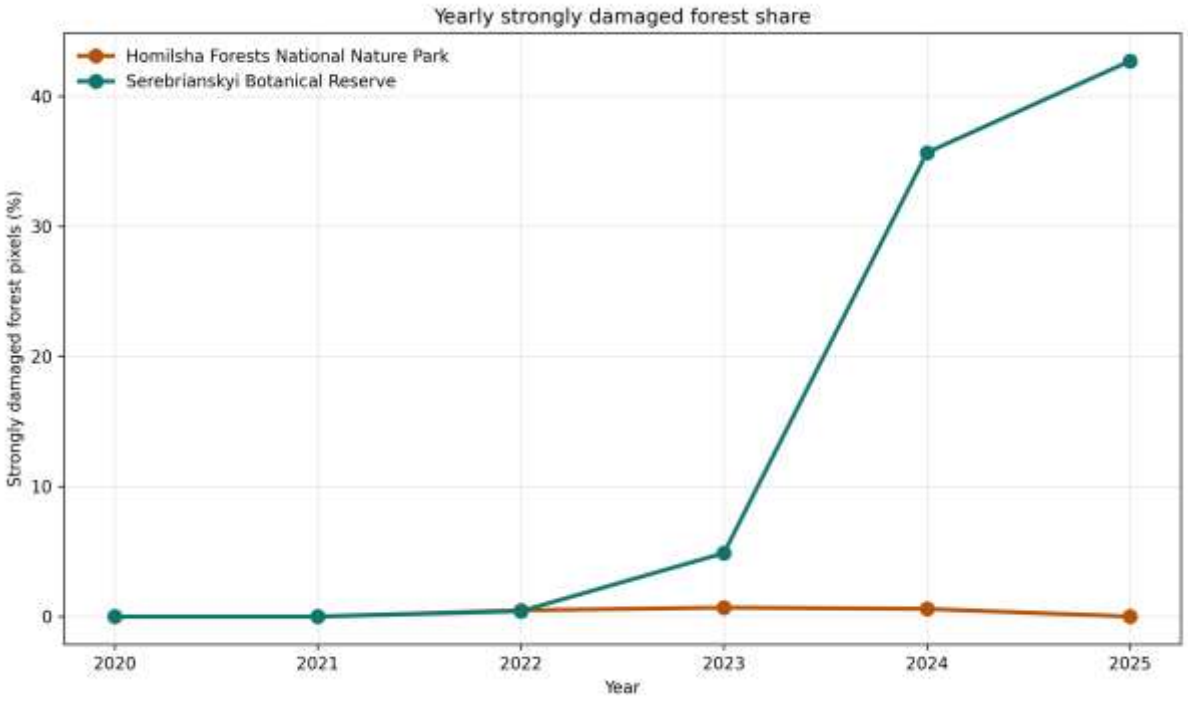

Fig. 8 – Annual share of destroyed forest pixels (%) in the conflict-affected Serebrianskyi Botanical Reserve and the control site in Homilsha Forests National Nature Park during 2020–2025

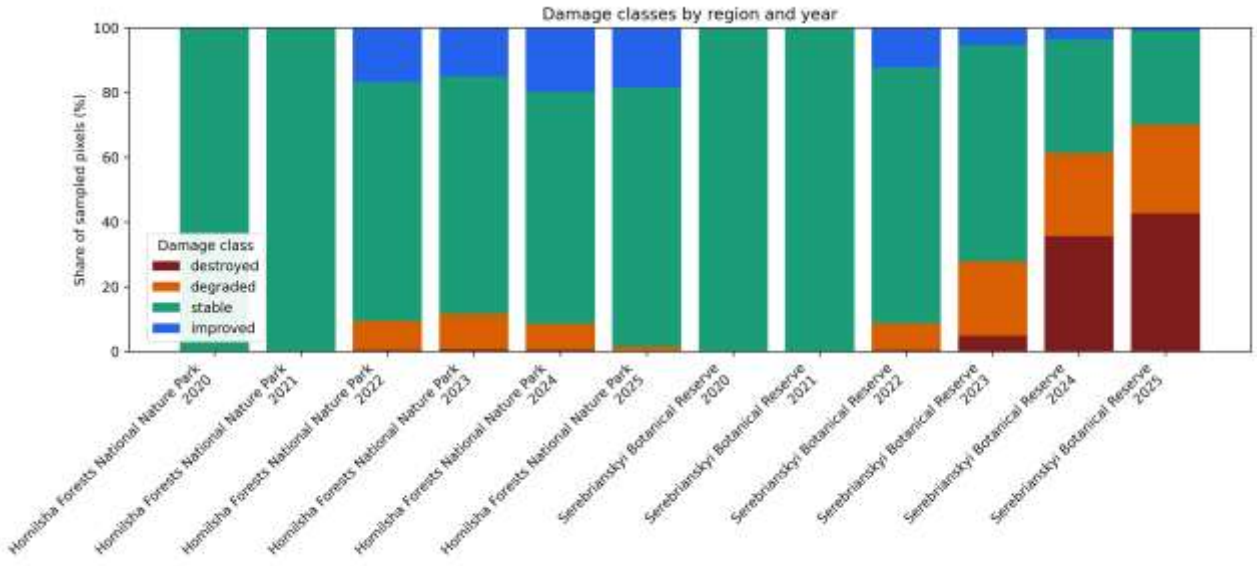

Fig. 9 – Annual distribution of forest damage classes in the conflict-affected Serebrianskyi Botanical Reserve and the control site in Homilsha Forests National Nature Park during 2020–2025

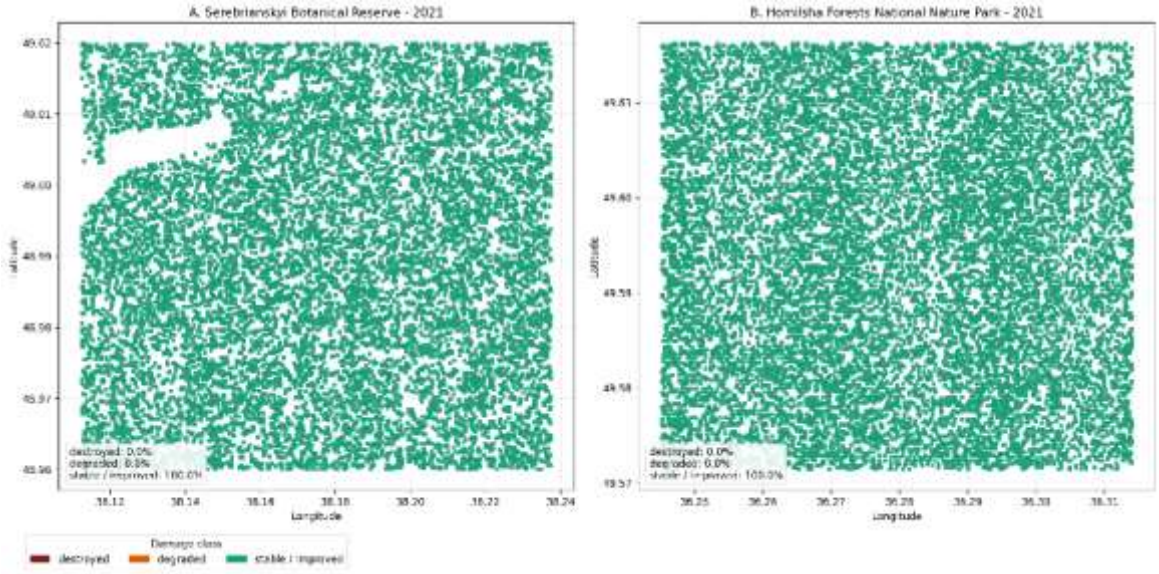

The left panel shows the Serebrianskyi Botanical Reserve, and the right panel shows Homilsha Forests National Nature Park. Colors indicate destroyed, degraded, and stable forest classes

Fig. 10 – Spatial distribution of forest disturbance classes in 2021

As shown in Figure 10, both forests remained spatially stable during the baseline period. No visible clusters of degraded or destroyed areas were present. This indicates that the disturbance pattern observed in later years was not present in the pre-disturbance period.

A different spatial pattern appeared after 2021. In 2022, disturbed areas were present in both AOIs, but they remained sparse and fragmented. In the Serebrianskyi Botanical Reserve, 8.7% of sampled forest area was classified as disturbed, including 8.3% degraded and 0.4% destroyed area. In the Homilsha control site, the disturbed share was 9.4%, including 8.9% degraded and 0.5% destroyed area. At this stage, disturbed areas in both sites were distributed as isolated points or small patches and did not form broad continuous zones. The spatial development from 2022 to 2025 is shown in Figure 11- 12.

In 2023, the spatial pattern in the Serebrianskyi Botanical Reserve changed substantially. The disturbed share increased to 27.9%, including 23.0% degraded and 4.9% destroyed area, while the share assigned to the stable/improved class decreased to 72.2%. Disturbed areas were no longer limited to isolated locations and began to form broader zones, especially in the central and southern parts of the AOI. In contrast, the Homilsha site remained dominated by the stable/improved class, which accounted for 88.4% of the sampled area. Although 11.6% of the area was classified as disturbed, these disturbed areas remained spatially dispersed and did not form large connected zones.

In 2024, the spatial expansion of disturbance in the Serebrianskyi Botanical Reserve became much stronger. The disturbed share reached 61.3%, including 25.6% degraded and 35.7% destroyed area, while the share assigned to the stable/improved class decreased to 38.7%. Large connected damaged zones became visible across a substantial part of the AOI. The spatial pattern changed from fragmented patches to broad continuous areas. In the Homilsha control site, the spatial pattern remained different. The stable/improved class accounted for 91.5% of the sampled area, while disturbed classes represented 8.5%, including 7.9% degraded and 0.6% destroyed area. These disturbed areas remained small and scattered In 2025, the spatial disturbance pattern in the Serebrianskyi Botanical Reserve intensified further. The disturbed share increased to 70.1%, including 27.4% degraded and 42.7% destroyed area, while the stable/improved class decreased to 29.9%. The destroyed class became the dominant disturbed category and occupied extensive connected zones across much of the AOI. Compared with 2023 and 2024, the 2025 pattern shows both further expansion and stronger spatial continuity of severe damage. In contrast, the Homilsha site remained almost entirely assigned to the stable/improved class. In 2025, 98.6% of the sampled area belonged to this class, 1.4% was classified as degraded, and no destroyed area was identified. The few disturbed

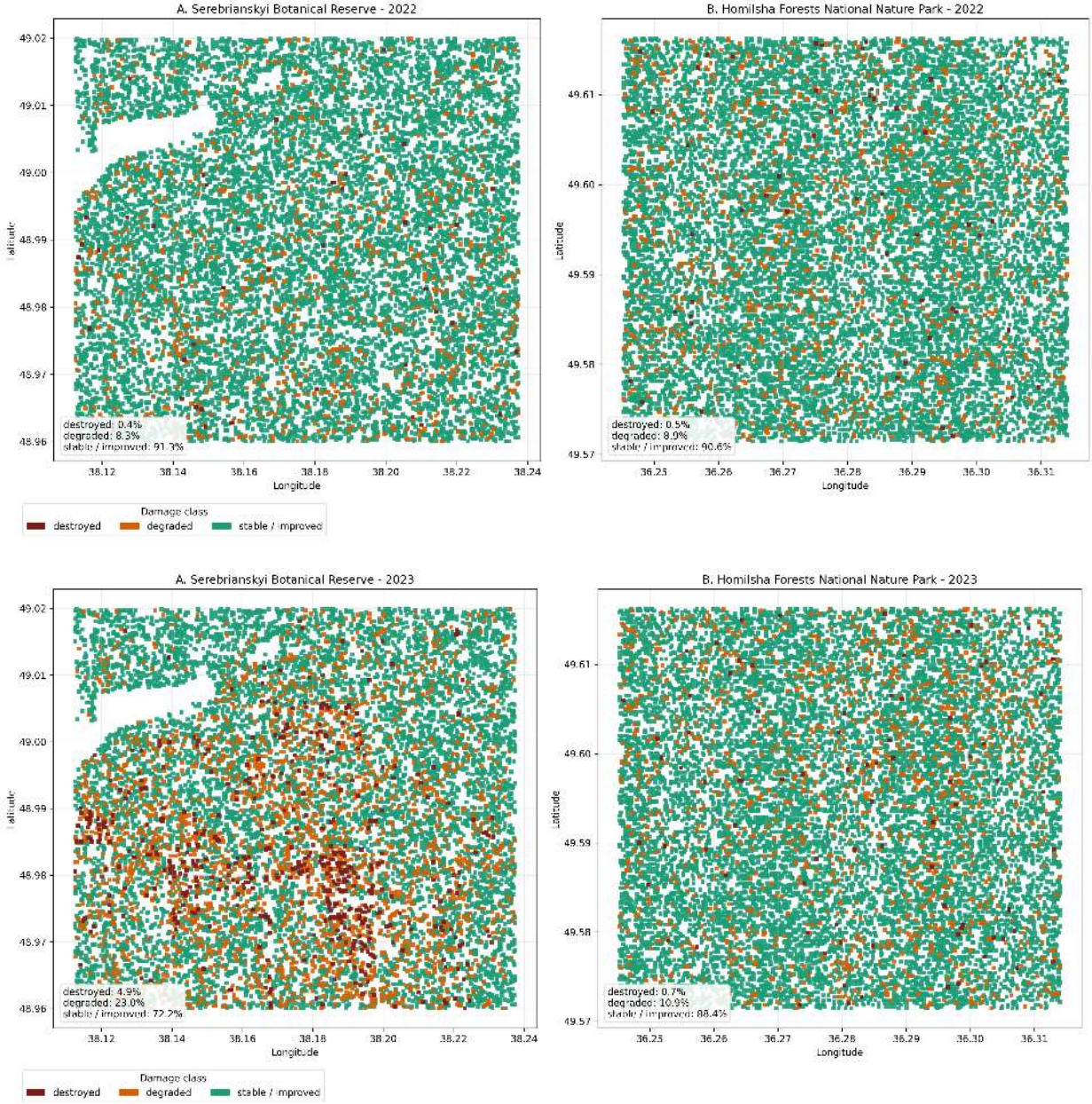

The left column shows the Serebrianskyi Botanical Reserve, and
the right column shows Homilsha Forests
National Nature Park.
From top to bottom, the rows correspond to 2024 and 2025.
Colors indicate destroyed, degraded, and stable/improved forest classes

Fig. 11 – Spatial distribution of forest disturbance classes in 2022–2023

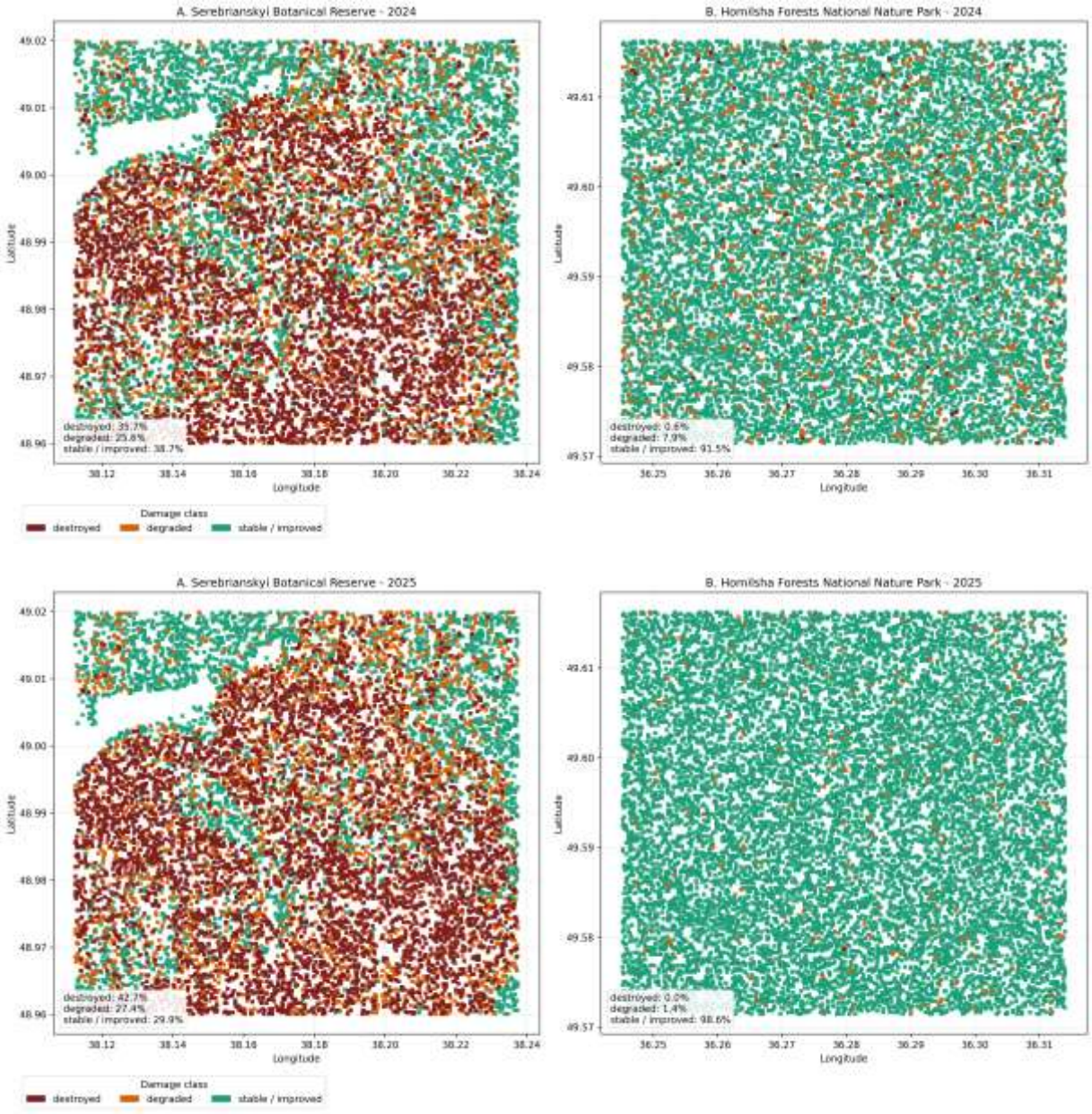

The left column shows the Serebrianskyi Botanical Reserve, and the right column shows Homilsha Forests National Nature Park. From top to bottom, the rows correspond to 2024 and 2025. Colors indicate destroyed, degraded, and stable/improved forest classes.

Fig. 12 - Spatial distribution of forest disturbance classes in 2024–2025

areas that remained were isolated and did not indicate broad spatial change.

Overall, the spatial maps show a transition in the Serebrianskyi Botanical Reserve from stable conditions in 2021 to sparse fragmented disturbance in 2022, broader disturbed zones in 2023, and extensive connected damaged areas in 2024–2025. The control forest did not show a comparable pattern and remained dominated by the stable/improved class throughout the study period. This result supports the interpretation that the disturbance signal in the conflict-affected forest reflects a real spatial expansion of forest damage rather than random variation.

Unsupervised classification reveals a gradient from intact to severely disturbed forest. The unsupervised classification separated the sampled forest pixels into four semantic classes: stable/intact forest, transitional/mixed forest,

degraded forest, and severely disturbed forest. This classification was based on multi-temporal Sentinel-1 features and allowed the forest condition to be represented as a gradient rather than as a binary damaged–undamaged pattern. As shown in Figure 13, the relative proportions of these classes differed strongly between the two study areas.

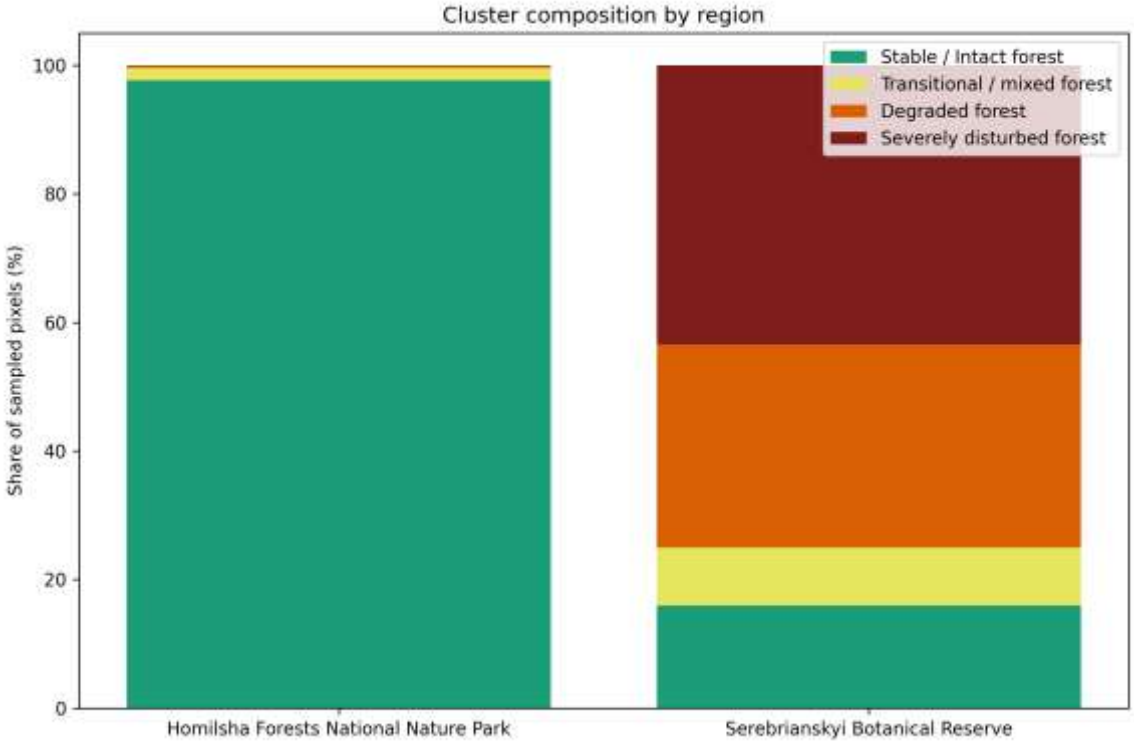

The classes include stable/intact forest, transitional/mixed forest, degraded forest, and severely disturbed forest

Fig. 13 – Composition of semantic forest-condition classes derived from K-means clustering in the Serebrianskyi Botanical Reserve and Homilsha Forests National Nature Park

The control site was dominated by the stable/intact class, which accounted for 97.7% of sampled pixels. The remaining classes represented only a small fraction of the area, including 1.9% transitional/mixed forest, 0.3% degraded forest, and 0.1% severely disturbed forest. In contrast, the Serebrianskyi Botanical Reserve showed a substantially different composition. Only 15.9% of sampled pixels were assigned to the stable/intact class, while 9.0% were classified as transitional/mixed, 31.6% as degraded, and 43.5% as severely disturbed. Thus, degraded and severely disturbed classes together accounted for 75.1% of the sampled forest in the conflict-affected site, compared with only 0.4% in the control site. The spatial distribution of these classes is shown in Figure 14.

The spatial pattern of the classes was also strongly different between the two study areas. In the Serebrianskyi Botanical Reserve, degraded and severely disturbed classes occupied large parts of the AOI and formed broad spatially continuous zones. The stable/intact class was restricted to a smaller proportion of the area and was spatially fragmented. The transitional/mixed class occupied an intermediate share and was located between the more stable and more disturbed parts of the AOI. In the Homilsha control site, the stable/intact class covered almost the entire sampled area, while the other classes appeared only as rare and isolated pixels without broad spatial continuity.

These results are consistent with the temporal and damage-class analyses presented in the previous sections. The conflict-affected forest was not only characterized by a larger damaged share, but also by a clear shift of the feature space toward degraded and severely disturbed conditions. In contrast, the control forest remained concentrated in the stable/intact class.

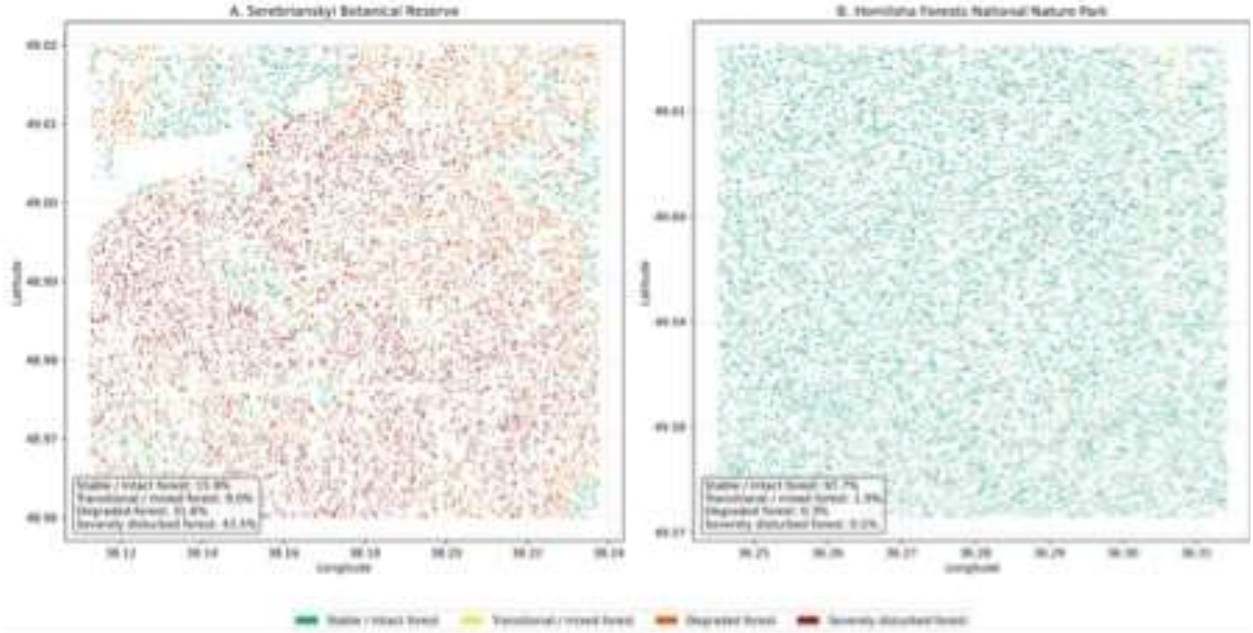

Colors indicate stable/intact forest, transitional/mixed forest, degraded forest, and severely disturbed forest

Fig. 14 – Spatial distribution of semantic forest-condition classes derived from K-means clustering in the Serebrianskyi Botanical Reserve and Homilsha Forests National Nature Park

Therefore, the unsupervised classification supports the interpretation that the disturbance signal is expressed as a continuous gradient of forest condition and not only as the presence or absence of damage. The main result is that the unsupervised classification clearly differentiated the conflict-affected forest from the control site and identified a strong predominance of degraded and severely disturbed classes in the Serebrianskyi Botanical Reserve.

Supporting anomaly detection and integrated evidence of forest disturbance. Anomaly detection provided additional support for the separation between the two study areas. Isolation Forest identified a substantially larger anomalous share in the conflict-affected Serebrianskyi Botanical Reserve than in the Homilsha control site. In the combined analysis, 22.8% of sampled pixels in Serebrianskyi were classified as anomalous, compared with 2.2% in Homilsha. This result indicates that the radar-temporal structure of the conflict-affected forest departed more strongly from the general pattern of forest condition represented in the full dataset (Tabl. 2).

This anomaly-based result is consistent with the main findings of the previous sections. The temporal analysis showed a progressive decline in RVI and backscatter in the Serebrianskyi forest relative to the 2020–2021 baseline, while the control site remained close to baseline or slightly positive. The damage classification showed a strong increase in disturbed forest area in Serebrianskyi, with the changed share reaching 70.1% and the destroyed share 42.7% in 2025. The spatial maps showed that

Table 2

Summary of anomaly detection results for the conflict-affected and control forest sites

Metric	Homilsha Forests National Nature Park	Serebrianskyi Botanical Reserve
n_pixels	12003	10934
anomaly_pixels	261	2492
mean_anomaly_score	0.42	0.48
median_anomaly_score	0.42	0.47
anomaly_share	0.02	0.23
run_name	combined	combined

this disturbance was not randomly distributed, but formed broad connected zones that expanded over time. In addition, the unsupervised classification showed that the conflict-affected AOI was dominated by degraded and severely disturbed classes, whereas the control site remained almost entirely within the stable/intact class.

Taken together, these results show agreement across several analytical levels. The conflict-affected forest showed a negative temporal shift in radar vegetation signal, a progressive increase in damaged area, a spatial expansion of connected disturbed zones, and a strong concentration of pixels assigned to degraded and severely disturbed classes. The control site did not show the same pattern. This overall agreement supports the interpretation that the observed changes in the Serebrianskyi Botanical Reserve reflect substantial forest disturbance rather than background variation.

Conflict-related disturbance signal in the Serebrianskyi forest. The results indicate that the forest disturbance signal observed in the Serebrianskyi Botanical Reserve is closely aligned with the spatial and temporal context of military activity in eastern Ukraine. The study area is located near the active frontline and was defined as a conflict-affected AOI exposed to warfare, military operations, and associated disturbances since 2022, while the Homilsha Forests National Nature Park was selected as a control site with lower exposure to direct military activity. This contrast provides an important interpretive basis for separating disturbance-related vegetation change from broader regional or seasonal variability.

The post-2022 decline in Sentinel-1 RVI, VV, and especially VH backscatter in the Serebrianskyi forest suggests a reduction in forest structural complexity. During the pre-disturbance period, the Serebrianskyi AOI showed relatively stable radar vegetation conditions, but after 2023 the RVI signal declined substantially and continued to decrease through 2024–2025. This decline was accompanied by reductions in both VV and VH backscatter, with a particularly strong decrease in the cross-polarized VH component. Because VH backscatter is more sensitive to volume scattering within vegetation canopies, its decline supports the interpretation that the observed signal reflects canopy degradation, loss of woody vegetation structure, or reduced vertical complexity rather than only short-term seasonal variation. This pattern is consistent with the expected effects of war-related disturbance on forest ecosystems. Shelling, explosions, fire events, movement of heavy military equipment, trenching, soil disturbance, fragmentation, and restricted forest management access can all contribute to canopy damage, tree mortality, exposure of bare or burned surfaces, and simplification of forest structure. Such processes would be expected to reduce vegetation-related volume scattering and therefore lower RVI and VH values. The sharp decline observed after 2022 is therefore not only temporally consistent with intensified military pressure, but also physically consistent with the way SAR signals respond to changes in vegetation structure. The comparison with the Homilsha control site strengthens this interpretation. Both AOIs were processed using the same Sentinel-1 data source, seasonal compositing window, forest mask, and baseline-relative workflow. However, the control forest did not show a comparable negative trend; instead, it remained stable or slightly positive relative to the baseline. Therefore, the divergence between the two forests indicates that the Serebrianskyi decline cannot be explained by regional seasonal variability alone. Rather, the combined decrease in RVI, VV, and VH points to a disturbance-driven structural change in the conflict-affected forest.

*Conflict-related disturbance signal in the Serebrianskyi forest.*The temporal pattern of disturbance in the Serebrianskyi Botanical Reserve suggests that the detected forest degradation was not a single short-term anomaly, but a progressive process that intensified after the beginning of large-scale military activity. During 2020–2021, both study areas remained close to baseline conditions, and no measurable damage signal was detected in either AOI. In 2022, disturbed pixels appeared in both regions, but the pattern was still limited and fragmented. This early-stage disturbance may reflect the initial emergence of abnormal vegetation signals, but it did not yet form a broad spatial pattern.

A clearer divergence became visible from 2023 onward. In the Serebrianskyi forest, the RVI deviation from the 2020–2021 baseline became negative in 2023 and then declined sharply in 2024–2025. The annual results show that RVI decreased by about 8.6% in 2023, 26.6% in 2024, and 28.7% in 2025 relative to the pre-disturbance baseline. The strongest shift occurred between 2023 and 2024, indicating that the main structural change in the vegetation signal developed after the initial phase of disturbance. In contrast, the Homilsha control site

remained stable or slightly positive during the same period, which strengthens the interpretation that the Serebrianskyi trajectory reflects localized disturbance pressure rather than a shared regional trend. The damage classification results confirm this cumulative pattern. In the Serebrianskyi AOI, the share of changed forest pixels increased from 8.7% in 2022 to 27.9% in 2023, then rose sharply to 61.3% in 2024 and 70.1% in 2025. The destroyed class followed an even stronger trajectory, increasing from only 0.4% in 2022 and 4.9% in 2023 to 35.7% in 2024 and 42.7% in 2025. This indicates that the disturbance did not only expand spatially, but also increased in severity. The shift from mostly stable forest conditions toward degraded and destroyed classes is consistent with prolonged and repeated disturbance rather than a temporary fluctuation in radar response.

The spatial maps further support this interpretation. In 2021, both AOIs were almost entirely stable or improved, with no visible clusters of degraded or destroyed forest. In 2022, disturbed pixels appeared as sparse and scattered patches in both sites. By 2023, however, the Serebrianskyi forest began to show broader disturbed zones, especially in the central and southern parts of the AOI. In 2024 and 2025, these areas expanded into large connected damaged zones, and the destroyed class became spatially dominant across much of the conflict-affected forest. The control site did not show a comparable spatial transition and remained dominated by stable or improved pixels throughout the same period. This temporal and spatial sequence is consistent with the effects of prolonged military pressure on forest ecosystems. Repeated shelling, fire events, mechanical disturbance from military equipment, trench construction, restricted access for forest management, and fragmentation of forest stands can gradually convert initially localized damage into broader structural degradation. The observed progression from sparse disturbance in 2022, to expanded degraded areas in 2023, and to extensive connected damaged zones in 2024–2025 therefore supports the interpretation that the Serebrianskyi forest experienced cumulative war-related disturbance over time.

Stability and slight improvement of the Homilsha control forest. The Homilsha Forests National Nature Park showed a markedly different temporal pattern from the conflict-affected Serebrianskyi forest. While the Serebrianskyi AOI experienced a sustained post-2022 decline in RVI and backscatter, the Homilsha control site remained comparatively stable throughout the observation period. Its RVI values did not show a negative trajectory; instead, they increased slightly from 0.72 in 2020 to 0.78 in 2025. The baseline-relative comparison also showed a positive deviation in later years, reaching approximately 5.1% in 2024 and 8.5% in 2025. This indicates that the control forest did not undergo the same structural degradation detected in the conflict-affected AOI. The damage classification results support this interpretation. In Homilsha, the share of changed forest pixels remained low and did not accumulate through time. Although 9.4% of pixels were classified as changed in 2022 and 11.6% in 2023, this share declined to 8.5% in 2024 and only 1.4% in 2025. The destroyed class remained negligible throughout the post-2022 period, with values of 0.5% in 2022, 0.7% in 2023, 0.6% in 2024, and 0.0% in 2025. Therefore, the control site showed only limited background variability rather than progressive degradation.

The slight positive shift in Homilsha may reflect several non-exclusive factors. It may be associated with natural interannual variability in vegetation condition, favorable moisture or growing-season conditions, or local ecological differences between the two forests. Homilsha is described as a mesophytic broadleaved and mixed forest system with a well-developed multi-layered structure, dense canopy, distinct shrub layer, and more favorable moisture conditions compared with the Serebrianskyi AOI. These structural and ecological characteristics may contribute to higher resilience of the radar vegetation signal and may partly explain why the site remained stable during the study period. Another plausible explanation is a temporary reduction in direct anthropogenic pressure during the war period. In protected or less accessible forest areas, reduced recreation, forestry operations, traffic, or other forms of human activity may allow vegetation structure to remain stable or show modest improvement. However, this interpretation should be treated carefully. The present analysis does not directly measure changes in forest management intensity, visitor pressure, local land use, or microclimatic conditions. Therefore, the observed positive RVI shift in Homilsha should not be interpreted as confirmed recovery, but rather as an indication that the control forest remained structurally stable or slightly improved according to Sentinel-1-derived indicators. Overall, the Homilsha site functions as an important reference for interpreting the Serebrianskyi disturbance signal.

Because both AOIs were analyzed using the same Sentinel-1 workflow, seasonal window, forest mask, baseline definition, and classification procedure, the absence of progressive degradation in Homilsha strengthens the conclusion that the strong decline and spatial expansion of damaged classes in Serebrianskyi were not caused by general regional variability alone. Instead, the contrast between the two sites supports the interpretation of localized disturbance pressure in the conflict-affected forest.

Methodological value, uncertainty, and implications for war-affected forest monitoring. The results show that Sentinel-1 SAR data, combined with baseline-relative change analysis and unsupervised machine learning, can provide a practical approach for monitoring forest disturbance in areas where field access is limited by military activity. The use of RVI, VV, and VH/VV indicators made it possible to detect both temporal decline and spatial expansion of damage in the Serebrianskyi forest, while the control site helped distinguish localized disturbance from broader regional variability.

However, the derived classes should be interpreted as remote-sensing-based indicators of structural disturbance rather than direct field-validated damage categories. SAR signals can be affected by canopy structure, moisture, surface roughness, fire effects, and acquisition conditions, and the two AOIs differ in vegetation composition and ecological context. Despite these uncertainties, the convergence of temporal, spatial, and machine learning evidence supports the usefulness of this workflow for rapid assessment and long-term monitoring of war-affected forests.

Conclusions

This study assessed forest disturbance in conflict-affected eastern Ukraine using Sentinel-1 SAR data, Radar Vegetation Index (RVI), baseline-relative change analysis, spatial classification, and unsupervised machine learning. Two forest areas were compared: the Serebrianskyi Botanical Reserve, located near the active frontline and exposed to military activity, and the Homilsha Forests National Nature Park, used as a control site with lower direct conflict exposure. Sentinel-1 VV and VH backscatter data for 2020–2025 were processed in Google Earth Engine, restricted to forest pixels, aggregated into summer seasonal composites, and compared against a 2020–2021 pre-disturbance baseline.

The results showed a clear post-2022 divergence between the two forests. In the Serebrianskyi AOI, RVI declined from stable pre-disturbance values of about 0.93–0.94 in 2020–2022 to 0.86 in 2023, 0.69 in 2024, and 0.67 in 2025. This decline was accompanied by decreases in both VV and VH backscatter, with the stronger reduction in VH indicating a loss of vegetation volume scattering and canopy structural complexity. In contrast, the Homilsha control site remained stable and showed a slight positive RVI shift, increasing from 0.72 in 2020 to 0.78 in 2025.

Baseline-relative analysis confirmed that the main disturbance signal in the Serebrianskyi forest emerged after 2022 and intensified in 2024–2025. RVI decreased by approximately 8.6% in 2023, 26.6% in 2024, and 28.7% in 2025 relative to the pre-disturbance baseline. The share of changed forest pixels increased from 8.7% in 2022 to 27.9% in 2023, 61.3% in 2024, and 70.1% in 2025. The destroyed class increased especially strongly, reaching 35.7% in 2024 and 42.7% in 2025. Spatial maps showed that this disturbance developed from sparse fragmented patches in 2022 into broad, connected damaged zones by 2024–2025.

Machine learning results supported the same interpretation. K-means clustering identified a strong predominance of degraded and severely disturbed classes in the Serebrianskyi forest, where these classes together accounted for 75.1% of sampled pixels. In contrast, the Homilsha control site was dominated by stable/intact forest, representing 97.7% of sampled pixels. Isolation Forest anomaly detection also showed a much higher anomalous share in Serebrianskyi than in Homilsha, further supporting the separation between the conflict-affected and control forests.

Tthe Serebrianskyi forest experienced a substantial and spatially expanding disturbance signal after 2022, consistent with the timing and location of prolonged military activity. The stability of the Homilsha control site cannot be explained by regional seasonal variability alone. Although the derived damage classes should be interpreted as remote-sensing-based indicators rather than field-validated damage categories, the convergence of temporal decline, spatial expansion, classification results, and anomaly detection supports the usefulness of Sentinel-1 RVI and SAR-based machine learning workflows for moni-toring war-affected forests where direct field access is limited.

Conflict of Interest

The authors certify that, although one of the authors of the article is a member of the editorial board of this journal, the peer review, publication decision, and editorial processes were conducted independently, without their participation or influence. Any potential conflicts of interest were fully mitigated through external oversight of the process.

Furthermore, the author has fully adhered to ethical norms, including avoiding plagiarism, data falsification, and duplicate publication.

Authors Contribution: all authors have contributed equally to this work

AI Statement

The authors used ChatGPT-5.5 (OpenAI, 2026) exclusively for language editing, structural organization of the text. All scientific content, materials and conclusions were created by the authors. All scientific statements, interpretations, results and conclusions have been critically reviewed by the authors, who bear full responsibility for the content of the manuscript.

References

1. Maksymenko, N. V., Voronin, V. O., & Burchenko, S. V. (2023). Remote Monitoring of the Impact of Military Actions on Forest Landscapes of the Kharkiv Region. *Man and Environment. Issues of Neoecology*, (40), 20–32. https://doi.org/10.26565/1992-4224-2023-40-02
2. Chornohor, L. F., Nekos, A. N., Titenko, H. V., & Chornohor, L. L. (2022). Mathematical Models for Assessing the Environmental Consequences of the Pyrogenic Factor Impact on Forest Ecosystems. *Visnyk of V. N. Karazin Kharkiv National University, Series "Ecology",* (27), 51–62. https://doi.org/10.26565/1992-4259-2022-27-04
3. Hanson, T. (2018). Biodiversity conservation and armed conflict: A warfare ecology perspective. *Annals of the New York Academy of Sciences,* 1429(1), 50–65. https://doi.org/10.1111/nyas.13689
4. Lawrence, M. J., Stemberger, H. L. J., Zolderdo, A. J., Struthers, D. P., & Cooke, S. J. (2015). The effects of modern war and military activities on biodiversity and the environment. *Environmental Reviews*, 23(4), 443–460. https://doi.org/10.1139/er-2015-0039
5. McNeely, J. A. (2003). Conserving forest biodiversity in times of violent conflict. *Oryx*, 37(2), 142–152. https://doi.org/10.1017/S0030605303000334
6. Mahreen, K. (2022). The environmental impacts of war and conflict. Institute of Development Studies. https://opendocs.ids.ac.uk/articles/report/The_Environmental_Impacts_of_War_and_Conflict/26427280
7. Gaynor, K. M., Fiorella, K. J., Gregory, G. H., Kurz, D. J., Seto, K. L., Withey, L. S., & Brashares, J. S. (2016). War and wildlife: Linking armed conflict to conservation. *Frontiers in Ecology and the Environment,* 14(10), 533–542. https://doi.org/10.1002/fee.1433
8. Ordway, E. M. (2015). Political shifts and changing forests: Effects of armed conflict on forest conservation in Rwanda. *Global Ecology and Conservation,* 3, 448–460. https://doi.org/10.1016/j.gecco.2015.01.013
9. Daiyoub, A., Gelabert, P., Saura-Mas, S., & Vega-García, C. (2023). War and deforestation: Using remote sensing and machine learning to identify the war-induced deforestation in Syria 2010–2019. *Land,* 12(8), 1509. https://doi.org/10.3390/land12081509
10. Butsic, V., Baumann, M., Shortland, A., Walker, S., & Kuemmerle, T. (2015). Conservation and conflict in the Democratic Republic of Congo: The impacts of warfare, mining, and protected areas on deforestation. *Biological Conservation*, 191, 266–273. https://doi.org/10.1016/j.biocon.2015.06.037
11. Kaplan, G., Rashid, T., Gasparović, M., & others. (2022). Monitoring war-generated environmental security using remote sensing: A review. *Land Degradation & Development.* https://doi.org/10.1002/ldr.4249
12. Shevchuk, S. A., Vyshnevskyi, V. I., & Bilous, O. P. (2022). The use of remote sensing data for investigation of environmental consequences of Russia–Ukraine war. *Journal of Landscape Ecology*, 15(3), 36–53. https://doi.org/10.2478/jlecol-2022-0017
13. Sticher, V., Wegner, J. D., & Pfeifle, B. (2023). Toward the remote monitoring of armed conflicts. *PNAS Nexus,* 2(6), pgad181. https://academic.oup.com/pnasnexus/article/2/6/pgad181/7185602
14. Mandal, D., Kumar, V., Ratha, D., Dey, S., Bhattacharya, A., Lopez-Sanchez, J. M., McNairn, H., & Rao, Y. S. (2020). Dual polarimetric radar vegetation index for crop growth monitoring using Sentinel-1 SAR data. *Remote Sensing of Environment,* 247, 111954. https://doi.org/10.1016/j.rse.2020.111954
15. Plank, S. (2014). Rapid damage assessment by means of multi-temporal SAR—A comprehensive review and outlook to Sentinel-1. *Remote Sensing,* 6(6), 4870–4906. https://doi.org/10.3390/rs6064870

16. Vreugdenhil, M., Wagner, W., Bauer-Marschallinger, B., Pfeil, I., Teubner, I., Rüdiger, C., & Strauss, P. (2018). Sensitivity of Sentinel-1 backscatter to vegetation dynamics: An Austrian case study. *Remote Sensing*, 10(9), 1396. https://doi.org/10.3390/rs10091396
17. Vreugdenhil, M., Navacchi, C., Bauer-Marschallinger, B., Hahn, S., Steele-Dunne, S., Pfeil, I., & Wagner, W. (2020). Sentinel-1 cross ratio and vegetation optical depth: A comparison over Europe. *Remote Sensing*, 12(20), 3404. https://doi.org/10.3390/rs12203404
18. De Luca, G., Silva, J. M. N., Di Fazio, S., & Modica, G. (2022). Integrated use of Sentinel-1 and Sentinel-2 data and open-source machine learning algorithms for land cover mapping in a Mediterranean region. *European Journal of Remote Sensing*, 55(1), 52–70. https://doi.org/10.1080/22797254.2021.2018667
19. Hirschmugl, M., Deutscher, J., Sobe, C., Bouvet, A., Mermoz, S., & Schardt, M. (2020). Use of SAR and optical time series for tropical forest disturbance mapping. *Remote Sensing*, 12(4), 727. https://doi.org/10.3390/rs12040727
20. Saim, A. A., & Aly, M. H. (2025). Fusion-based approaches and machine learning algorithms for forest monitoring: A systematic review. *Wild*, 2(1), 7. https://www.mdpi.com/3042-4526/2/1/7
21. Gatti, R. C., Lobos, R. B. C., Torresani, M., & others. (2025). An early warning system based on machine learning detects huge forest loss in Ukraine during the war. *Global Ecology and Conservation*. https://www.sciencedirect.com/science/article/pii/S2351989425000289
22. Mullissa, A., Reiche, J., & Herold, M. (2023). Deep learning and automatic reference label harvesting for Sentinel-1 SAR-based rapid tropical dry forest disturbance mapping. *Remote Sensing of Environment*. https://www.sciencedirect.com/science/article/pii/S0034425723003504
23. Xu, C., Ding, Y., Zheng, X., Wang, Y., Zhang, R., Zhang, H., & others. (2022). Comparison of machine learning and feature selection methods for maize biomass estimation using Sentinel-1 SAR, Sentinel-2 vegetation indices, and biophysical variables. *Remote Sensing*, 14(16), 4083. https://doi.org/10.3390/rs14164083

Submission received: 03.04.2026 / Revised: 04.05.2026 /Accepted: 08.05.2026 / Published: 30.05.2026

Л. А. ГОРОШКОВА, д-р екон. наук, проф.,
Професор кафедри екології
e-mail: goroshkova69@gmail.com ORCID ID: https://orcid.org/0000-0002-7142-4308
Національний університет «Києво-Могилянська академія»
вул. Сковороди, 2, Київ, 04070, Україна

О. І. МЕНЬШОВ, д-р геол. наук,
Старший науковий співробітник кафедри геоінформатики
e-mail: menshov@knu.ua ORCID ID: https://orcid.org/0000-0001-7280-8453
Київський національний університет імені Тараса Шевченка
вул. Володимирська, 60, Київ, 01033, Україна

Д. В. МАСЛОВ,
Аспірант кафедри екології
e-mail: 20denismaslov@gmail.com ORCID ID: https://orcid.org/0009-0009-7397-8329
Національний університет «Києво-Могилянська академія»
вул. Сковороди, 2, Київ, 04070, Україна

ОЦІНКА ВІЙСЬКОВИХ ВПЛИВІВ НА ПРИРОДООХОРОННІ ТЕРИТОРІЇ УКРАЇНИ ЗА ДОПОМОГОЮ SENTINEL-1 ТА МАШИННОГО НАВЧАННЯ

Мета. Оцінити військові впливи на природоохоронні території України за допомогою даних Radar Vegetation Index (RVI) Sentinel-1 та методів машинного навчання з метою виявлення просторових і часових закономірностей порушення рослинності та трансформації екосистем в умовах воєнного часу.

Методи. Просторові та часові зміни аналізувалися із застосуванням методів дистанційного зондування Землі у поєднанні з методами машинного навчання, зокрема алгоритмами неконтрольованої класифікації для виявлення закономірностей порушення рослинності та трансформації

екосистем. Додатково застосовано порівняльний аналіз і аналіз часових рядів для оцінки впливу військової діяльності на лісові екосистеми в умовах воєнного часу.

Результати. Оцінено вплив військової діяльності на лісові екосистеми сходу України з використанням даних Sentinel-1 SAR, індексу рослинності Radar Vegetation Index (RVI), аналізу змін відносно базового періоду та методів неконтрольованого машинного навчання. Кількісна оцінка та характеристика порушень лісових екосистем, пов'язаних із воєнними діями, у межах Серебрянського ботанічного заказника, який безпосередньо зазнає впливу активних бойових дій, а також визначення масштабів, інтенсивності та часової динаміки цих пошкоджень визначено відносно довоєнного базового періоду, для чого використовувалася контрольна територія – Національний природний парк «Гомільшанські ліси», який не зазнавав впливу бойових дій. Оцінено, наскільки показники Sentinel-1 RVI, а також коефіцієнти зворотного розсіювання VV і VH здатні відображати просторові закономірності та поступовий розвиток порушень лісів, спричинених військовими діями, протягом 2020–2025 років. Дані Sentinel-1 оброблялися у середовищі Google Earth Engine та були обмежені лише лісовими пікселями за допомогою маски земного покриву. Для кожного року були сформовані літні композити, а довоєнний базовий період (2020–2021 роки) використовувався для кількісної оцінки післявоєнних змін. Аналіз включав оцінку річних трендів RVI, класифікацію пошкоджень на основі правил, кластеризацію методом K-means та виявлення ізольованих аномалій лісового покриву. Після 2022 року до 2025 року в межах Серебрянської дослідної території (ROI) зафіксовано суттєве зниження значень RVI. Частка змінених лісових пікселів значно збільшена, зокрема частка сильно порушених пікселів також значно збільшилася. Водночас у межах Гомільшанської дослідної території (ROI) зберігалася стабільна ситуація. Результати машинного навчання підтвердили ці тенденції.

Висновки. Методи SAR продемонстрували високу ефективність для дистанційного моніторингу в умовах обмеженого польового доступу, однак отримані категорії пошкоджень слід розглядати як індикатори дистанційного зондування, а не як польово підтверджені категорії деградації екосистем.

КЛЮЧОВІ СЛОВА: *Sentinel-1, SAR, Radar Vegetation Index, порушення лісів, умови лісів, дистанційне зондування Землі, машинне навчання*

Конфлікт інтересів

Автори засвідчують, що, незважаючи на те, що один із авторів статті є членом редакційної колегії цього журналу, процес рецензування, прийняття рішення щодо публікації та редагування проводилися незалежно, без його участі чи впливу. Будь-які потенційні конфлікти інтересів були повністю усунені шляхом зовнішнього контролю процесу.

Крім того, автори повністю дотримувались етичних норм, включаючи плагіат, фальсифікацію даних та подвійну публікацію.

Внесок авторів. Автори зробили рівний внесок в це дослідження.

Декларація про використання ШІ

Автори використовували ChatGPT-5.5 (OpenAI, 2026) виключно для мовного редагування, структурного впорядкування тексту. Весь науковий контент, матеріали та висновки створені авторами. Усі наукові положення, інтерпретації, результати та висновки критично перевірені авторами, які несуть повну відповідальність за зміст рукопису.

Список використаної літератури

1. Максименко , Н. В., Воронін , В. О., Бурченко , С. В. Дистанційний моніторинг впливу військових дій на лісові ландшафти Харківської області . *Людина та довкілля. Проблеми неоекології*. 2023. Вип. 40. С. 20-32. https://doi.org/10.26565/1992-4224-2023-40-02
2. Чорногор, Л. Ф., Некос, А. Н., Тітенко, Г. В., Чорногор, Л. Л. Математичні моделі для оцінки екологічних наслідків впливу пірогенного фактору на лісові екосистеми. *Вісник Харківського національного університету імені В. Н. Каразіна серія «Екологія»*. 2022. Вип.27. С.51-62. https://doi.org/10.26565/1992-4259-2022-27-04
3. Hanson, T. Biodiversity conservation and armed conflict: A warfare ecology perspective. *Annals of the New York Academy of Sciences*. 2018. Vol. 1429. No 1. P.50–65. https://doi.org/10.1111/nyas.13689

4. Lawrence, M. J., Stemberger, H. L. J., Zolderdo, A. J., Struthers, D. P., Cooke, S. J. The effects of modern war and military activities on biodiversity and the environment. *Environmental Reviews.* 2015. Vol. 23. No 4. P. 443–460. https://doi.org/10.1139/er-2015-0039
5. McNeely, J. A. Conserving forest biodiversity in times of violent conflict. *Oryx*. 2003. Vol. 37. No 2. P. 142–152. https://doi.org/10.1017/S0030605303000334
6. Mahreen, K. The environmental impacts of war and conflict. Institute of Development Studies. 2022. https://open-docs.ids.ac.uk/articles/report/The_Environmental_Impacts_of_War_and_Conflict/26427280
7. Gaynor, K. M., Fiorella, K. J., Gregory, G. H., Kurz, D. J., Seto, K. L., Withey, L. S., Brashares, J. S. War and wildlife: Linking armed conflict to conservation. *Frontiers in Ecology and the Environment*. 2016. Vol.14. No 10. P. 533–542. https://doi.org/10.1002/fee.1433
8. Ordway, E. M. Political shifts and changing forests: Effects of armed conflict on forest conservation in Rwanda. *Global Ecology and Conservation*. 2015. Vol.3. P.448–460. https://doi.org/10.1016/j.gecco.2015.01.013
9. Daiyoub, A., Gelabert, P., Saura-Mas, S., Vega-García, C. War and deforestation: Using remote sensing and machine learning to identify the war-induced deforestation in Syria 2010–2019. *Land*. 2023. Vol. 12. No 8. P. 1509. https://doi.org/10.3390/land12081509
10. Butsic, V., Baumann, M., Shortland, A., Walker, S., Kuemmerle, T. Conservation and conflict in the Democratic Republic of Congo: The impacts of warfare, mining, and protected areas on deforestation. *Biological Conservation*. 2015. Vol. 191. P. 266–273. https://doi.org/10.1016/j.biocon.2015.06.037
11. Kaplan, G., Rashid, T., Gasparović, M., & others. Monitoring war-generated environmental security using remote sensing: A review. *Land Degradation & Development.* 2022. https://doi.org/10.1002/ldr.4249
12. Shevchuk, S. A., Vyshnevskyi, V. I., Bilous, O. P. The use of remote sensing data for investigation of environmental consequences of Russia–Ukraine war. *Journal of Landscape Ecology*. 2022. Vol. 15. No 3. P. 36–53. https://doi.org/10.2478/jlecol-2022-0017
13. Sticher, V., Wegner, J. D., Pfeifle, B. Toward the remote monitoring of armed conflicts. *PNAS Nexus*. 2023. Vol. 2. No 6. pgad181. https://academic.oup.com/pnasnexus/article/2/6/pgad181/7185602
14. Mandal, D., Kumar, V., Ratha, D., Dey, S., Bhattacharya, A., Lopez-Sanchez, J. M., McNairn, H., Rao, Y. S. Dual polarimetric radar vegetation index for crop growth monitoring using Sentinel-1 SAR data. *Remote Sensing of Environment*, 2020. Vol. 247. 111954. https://doi.org/10.1016/j.rse.2020.111954
15. Plank, S. Rapid damage assessment by means of multi-temporal SAR—A comprehensive review and outlook to Sentinel-1. *Remote Sensing.* 2014. Vol. 6(6. P. 4870–4906. https://doi.org/10.3390/rs6064870
16. Vreugdenhil, M., Wagner, W., Bauer-Marschallinger, B., Pfeil, I., Teubner, I., Rüdiger, C., Strauss, P. Sensitivity of Sentinel-1 backscatter to vegetation dynamics: An Austrian case study. *Remote Sensing*. 2018. Vol.10. No 9. P. 1396. https://doi.org/10.3390/rs10091396
17. Vreugdenhil, M., Navacchi, C., Bauer-Marschallinger, B., Hahn, S., Steele-Dunne, S., Pfeil, I., & Wagner, W. Sentinel-1 cross ratio and vegetation optical depth: A comparison over Europe. *Remote Sensing*. 2020. Vol.12(20. P. 3404. https://doi.org/10.3390/rs12203404
18. De Luca, G., Silva, J. M. N., Di Fazio, S., Modica, G. Integrated use of Sentinel-1 and Sentinel-2 data and open-source machine learning algorithms for land cover mapping in a Mediterranean region. *European Journal of Remote Sensing*. 2022. Vol. 55. No 1. P.52–70. https://doi.org/10.1080/22797254.2021.2018667
19. Hirschmugl, M., Deutscher, J., Sobe, C., Bouvet, A., Mermoz, S., Schardt, M. Use of SAR and optical time series for tropical forest disturbance mapping. *Remote Sensing*. 2020. Vol.12. No 4. P. 727. https://doi.org/10.3390/rs12040727
20. Saim, A. A., Aly, M. H. Fusion-based approaches and machine learning algorithms for forest monitoring: A systematic review. *Wild.* 2025. Vol. 2. No 1. P. 7. URL: https://www.mdpi.com/3042-4526/2/1/7
21. Gatti, R. C., Lobos, R. B. C., Torresani, M., & others. An early warning system based on machine learning detects huge forest loss in Ukraine during the war. Global Ecology and Conservation. 2025. URL: https://www.sciencedirect.com/science/article/pii/S2351989425000289
22. Mullissa, A., Reiche, J., Herold, M. Deep learning and automatic reference label harvesting for Sentinel-1 SAR-based rapid tropical dry forest disturbance mapping. *Remote Sensing of Environment*. 2023. URL: https://www.sciencedirect.com/science/article/pii/S0034425723003504
23. Xu, C., Ding, Y., Zheng, X., Wang, Y., Zhang, R., Zhang, H., & others. Comparison of machine learning and feature selection methods for maize biomass estimation using Sentinel-1 SAR, Sentinel-2 vegetation indices, and biophysical variables. *Remote Sensing*. 2022. Vol. 14. . No 16. P.4083. https://doi.org/10.3390/rs14164083

Отримано: 03.04.2026 / Переглянуто: 04.05.2026 / Прийнято: 08.05.2026 / Опубліковано: 30.05.2026